universität wien

DIPLOMARBEIT

Titel der Diplomarbeit

„Bindungsstudien zur Selektivitätsbestimmung von Adenosin-Rezeptor-Liganden“

verfasst von

Theresa Balber

angestrebter akademischer Grad

Magistra der Pharmazie (Mag.pharm.)

Wien, 2014

Studienkennzahl lt. Studienblatt:	A 449
Studienrichtung lt. Studienblatt:	Diplomstudium Pharmazie
Betreut von:	o. Univ.-Prof. Mag. Dr. Helmut Viernstein

ACKNOWLEDGEMENT

First of all, I would like to express my sincere gratitude to O. Univ.-Prof. Mag. Dr. Helmut Viernstein for supervising my thesis.

I would like to thank the head of the division of nuclear medicine, Univ.-Prof. Dr. Marcus Hacker, as well as Prof. Mag. Dr. Markus Mitterhauser and Prof. Mag. Dr. Wolfgang Wadsak for providing the facilities that enabled this thesis. My personal thanks to Markus Mitterhauser, who inspired me for the field of radiopharmacy during his lecture some years ago. Thank you for offering me such an interesting topic and for your helpful advice.

I would like to thank Mag. Dr. Daniela Häusler for all the time she has spent on correcting my thesis. Thank you for all the discussing, listening and giving advice during the whole time we were working together. Thanks a lot for your encouraging words, when nothing worked out.

Furthermore, I want to thank my colleagues for welcoming me in their team and always offering me a helping hand.

I am deeply grateful to my parents for their continuous support and motivation throughout my studies.

ABSTRACT (ENGLISH)

Adenosine is an important modulator in the energy homeostasis of the human body and acts through four different adenosine receptor subtypes, denoted as A1, A2A, A2B and A3 receptors. Since the adenosine A3 receptor (A3R) is highly expressed in primary and metastatic tumors (human melanoma, colon, breast, small-cell lung cancer, pancreatic carcinoma tissues and lymph node metastasis) versus non-neoplastic tissue it is a potent target for molecular imaging of tumor-related pathologies.

Aim of this thesis was the *in-vitro* evaluation of several new FE@SUPPY-derivatives (FE^2@SUPPY, Me^2@SUPPY, FEMe@SUPPY:2 and FE@SUPPY:11) regarding their respective affinities for different adenosine receptor subtypes (hA1R, hA2AR, hA3R). Hence selectivity for the A3R subtype was calculated to identify highly selective A3R antagonists with the potential to serve as future PET-tracers. Apart from that, structurally related ligands (FE@CAPPY and Me^2@CAPPY) as well as structurally different compounds (BD1 and BD3) were investigated. Furthermore, binding profiles of the respective metabolites of the PET-tracers [^{18}F]FE@SUPPY and [^{18}F]FE@SUPPY:2, DFE@SUPPY and DFE@SUPPY:2, were evaluated. Moreover, selectivity of the lead compounds, the A3R antagonists FE@SUPPY and FE@SUPPY:2, was determined and verified. Their binding profiles were compared with (1) the new ligands and (2) the A3R antagonists MRS1191 and MRS1523.

Radioligand binding assays were performed using a Brandel® cell harvester. Competition experiments were conducted using membranes expressing hA1R, hA2AR and hA3R and [^{3}H]DPCPX, [^{3}H]CGS21680 or [^{125}I]AB-MECA as radioligands, respectively. Depending on the receptor assay conditions varied in incubation time, composition of buffer and additives (BSA, ADA). Radioactivity was detected by liquid scintillation counting or gamma-counting. Data were evaluated (competitive binding curves were generated for determination of IC_{50} values) using the GraphPad Prism® Software (San Diego, version 5). K_i values were calculated via the Cheng and Prusoff equation.

BD1, BD3, FE@SUPPY:11, DFE@SUPPY and DFE@SUPPY:2 showed human A3R K_i values in a µM range; FE@CAPPY, Me^2@CAPPY, Me^2@SUPPY and FEMe@SUPPY:2 showed intermediate

to low affinity for the hA3R. These compounds are therefore not suitable as potential PET-tracers. FE^2@SUPPY turned out as a potential candidate, since it shows high affinity for the hA3R and good selectivity towards the other adenosine subtypes. However, FE@SUPPY shows the best binding profile among all tested compounds, displaying high affinity for the hA3R (K_i=6.02nM±0.4) and good selectivity towards the other subtypes with ratios of 1/669 (hA1R/hA3R) and 1/286 (hA2AR/hA3R).

A positive finding regarding the pharmacokinetics of [^{18}F]FE@SUPPY and [^{18}F]FE@SUPPY:2 is that the respective metabolites DFE@SUPPY and DFE@SUPPY:2 do not show any affinity for the hA3R. This thesis confirmed once more the potential of FE@SUPPY to serve as a future PET-tracer, as it displays an outstanding binding profile among a pool of new derivatives.

ABSTRACT (DEUTSCH)

Adenosin spielt eine zentrale Rolle in der Energiehomöostase des menschlichen Körpers. Physiologisch wirkt es über vier verschiedene Rezeptoren, die als Adenosin-A_1-Rezeptor (A1R), Adenosin-A_{2A}-Rezeptor (A2AR), Adenosin-A_{2B}-Rezeptor (A2BR) und Adenosin-A_3-Rezeptor (A3R) bezeichnet werden. Da der A3R von primären (humanes Melanom, Dickdarm-, Brust-, Kleinzelliges Lungen- und Pankreaskarzinom) und metastasierenden Tumoren (Lymphknotenmetastasen) vermehrt exprimiert wird, im Vergleich zu gesundem, nicht neoplastischem Gewebe, stellt der A3R ein potentielles Target für die Bildgebung von Tumorerkrankungen dar.

Ziel dieser Diplomarbeit war die *in-vitro* Evaluierung neuer FE@SUPPY-Derivate (FE^2@SUPPY, Me^2@SUPPY, FEMe@SUPPY:2 und FE@SUPPY:11) hinsichtlich deren Affinität zu den Adenosin-Rezeptor-Subtypen A1R, A2AR und A3R. In weiterer Folge wurde deren Selektivität hinsichtlich des A3R bestimmt, um potentielle hoch affine und selektive A3R Antagonisten, als zukünftige A3R PET-Tracer, zu identifizieren. Des Weiteren wurden strukturell ähnliche (FE@CAPPY, Me^2@CAPPY) wie auch strukturell andersartige Verbindungen (BD1, BD3) evaluiert. Zudem wurden die Bindungsprofile der entsprechenden Metaboliten der beiden PET-Tracer, [^{18}F]FE@SUPPY und [^{18}F]FE@SUPPY:2, DFE@SUPPY und DFE@SUPPY:2, untersucht. Darüber hinaus wurde die Selektivität der A3R Antagonisten FE@SUPPY und FE@SUPPY:2 bestimmt und verifiziert. Deren Bindungsprofile wurden anschließend (1) mit den neuen Liganden und (2) mit den A3R Antagonisten MRS1523 und MRS1191 verglichen.

Die Radioliganden-Bindungs-Experimente wurden mit Hilfe eines Brandel® Cell Harvesters durchgeführt. Die Verdrängungsexperimente erfolgten mittels Membranen, die den gewünschten Rezeptor (hA1R, hA2AR und hA3R) exprimieren, und mittels [^{3}H]DPCPX, [^{3}H]CGS21680 oder [^{125}I]AB-MECA als entsprechende Radioliganden. Abhängig von dem verwendeten Rezeptor unterschieden sich die Versuchsbedingungen in der Inkubationszeit, dem verwendeten Puffer und Pufferzusätzen (ADA, BSA). Die Radioaktivität wurde mittels Flüssigszintillation beziehungsweise Messung der Gammastrahlung bestimmt. Die Datenauswertung (Generierung der kompetitiven Verdrängungskurven und Ermittlung der

IC_{50}-Werte) erfolgte mit Hilfe der GraphPad Prism® Software (San Diego, Version 5). Die K_i-Werte wurden mittels der Gleichung nach Cheng und Prusoff berechnet.

BD1, BD3, FE@SUPPY:11, DFE@SUPPY und DFE@SUPPY:2 zeigten K_i-Werte für den humanen A3R im µM-Bereich. FE@CAPPY, Me^2@CAPPY, Me^2@SUPPY und FEMe@SUPPY:2 zeigten mittlere bis niedrige Affinität für den humanen A3R. Diese Komponenten sind daher nicht geeignet als zukünftige PET-Tracer. FE^2@SUPPY stellt einen potentiellen neuen A3R PET-Tracer Kandidaten dar, da es hohe Affinität zu dem hA3R wie auch gute Selektivität gegenüber den anderen Subtypen aufweist. FE@SUPPY zeigt das beste Bindungsprofil unter all den getesteten Komponenten, da es durch eine hohe Affinität für den hA3R (K_i=6.02nM±0.4) als auch durch eine hohe Selektivität gegenüber den anderen Subtypen mit Verhältnissen von 1/669 (hA1R/hA3R) und 1/286 (hA2AR/hA3R) ausgezeichnet ist.

Eine positive Erkenntnis dieser Studie betreffend der Pharmakokinetik der PET-Tracer [^{18}F]FE@SUPPY und [^{18}F]FE@SUPPY:2 war, dass die entsprechenden Metaboliten DFE@SUPPY und DFE@SUPPY:2 keine Affinität am hA3R zeigten.

Diese Diplomarbeit bestätigt ein weiteres Mal das Potential von FE@SUPPY als A3R PET-Tracer zu dienen, da es ein sehr gutes Bindungsprofil aufweist.

CONTENT

1 INTRODUCTION

1.1. ADENOSINE

The adenosine receptor is named after its physiological endogenous ligand, the purine nucleoside adenosine (see Figure 1). Adenosine is ubiquitary present in every cell and a part of energy-providing nucleotides and nucleic acids. [1]

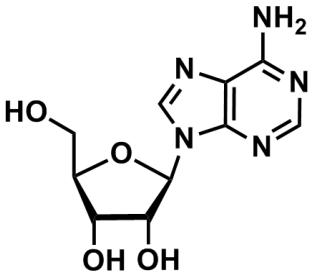

Figure 1: Chemical structure of adenosine: it comprises the purine base adenine and a ribose sugar molecule, which is attached to N9

As an autacoid, adenosine is characterized by a brief physiological lifetime and acts locally in contrast to hormones which are characterized by systemic effects. In the extracellular space, adenosine is generated by hydrolysis of adenine nucleotides as the breakdown of ATP through ectoenzymes (apyrase CD39, ecto-5´-nucleotidase CD73). The conversion of AMP to adenosine, carried out by CD73, represents the limiting step for its formation. The intracellular formation of adenosine is mediated either by dephosphorylation of AMP or by hydrolysis of S-adenosyl-homocysteine. Adenosine is unstable as it is rapidly degraded by deamination or cellular reuptake. It is phosphorylated by adenosine kinase to AMP or to a lesser extent degraded by adenosine deaminase to inosine (see Figure 2). Both metabolites are less active than adenosine at the respective adenosine receptors (ARs). [2],[3]

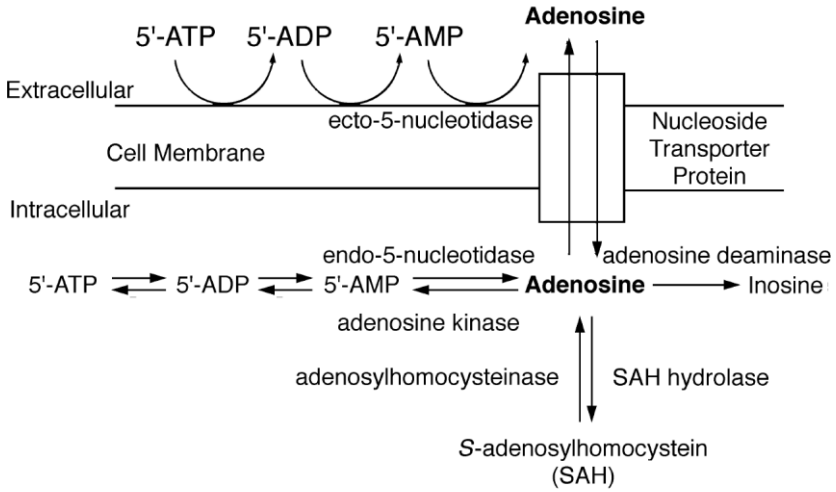

Figure 2: Pathways of adenosine metabolism (biosynthesis and degradation) and transport [1]

Under basal conditions, extracellular adenosine concentrations are about 100nM in the heart and 20nM in the brain which lead to only a partial activation of ARs. Extracellular adenosine levels can rapidly rise to micromolar range, which cause a generalized activation of ARs. This happens as a response to stress to an organ or tissue or as a result of increased metabolic rates. Adenosine either reduces the energy demand or increases the energy supply of an organ and therefore it holds a key role in energy homeostasis. Moreover, extracellular adenosine acts as a cytoprotective modulator by increasing blood supply via vasodilatation, suppressing inflammation and/ or ischemic preconditioning. For example, large amounts of adenosine are released during myocardial ischemia, resulting in effective preconditioning of cardiomyocytes. [2]

1.1.1. THE ADENOSINE RECEPTOR FAMILY

Adenosine exerts many physiological functions in the body by acting on cell surface receptors coupling to intracellular signaling pathways. To date, there are 4 known subtypes of the adenosine receptor, denoted as adenosine A_1 receptor (A1R), adenosine A_{2A} receptor (A2AR), adenosine A_{2B} receptor (A2BR) and adenosine A_3 receptor (A3R). Each exhibits a unique pharmacological profile, as well as tissue distribution, effector coupling and ligand affinity. Adenosine shows different affinity towards the adenosine receptor subtypes; lowest affinity for the A2BR (K_i>1µM), whereas highest affinity for A2AR and A1R (K_i values in binding of 10-30nM at the high affinity sites) and intermediate affinity for A3R (ca. 1µM for rA3R). [2]

All AR-subtypes are members of the superfamily of G protein coupled receptors (GPCRs), which comprise seven transmembrane regions, located on the cell surface. Based on amino acid sequence similarity, seven families of GPCRs can be distinguished. The main family (family A) comprises the majority of GPCRs, as rhodopsin, adrenoceptors and the adenosine receptors. [4]

Representatively for GPCRs, a single polypeptid chain forms a central core domain that consists of seven transmembrane helices (TM1-7), which are connected by three intracellular (IL1-3) and three extracellular loops (EL1-3). The N-terminus is located in the extracellular space and the C-terminus in the cytosol. Sites for posttranslational modifications, such as glycosylation can be found in the extracellular domains and moreover, sites for palmitoylation can be found within the C-terminal domains of A1R and A3R. The A2AR features a long C-terminal segment, which counts more than 120 amino acid residues and can serve as a binding site for so-called accessory proteins. [2]

Stimulation of A1R and A3R causes inhibition of the adenylate cyclase by coupling to the inhibiting G protein (G_i). However, the A2Rs are coupled to the stimulating G protein (G_s), leading to a stimulation of adenylate cyclase, respectively. The A3 and A2B receptors are coupled to G_q, resulting in a stimulation of phospholipase C (PLC) and release of the second messenger molecules diacylglycerol (DAG) and inositol (1,4,5)-triphosphate (IP_3), which regulate protein kinase C (PKC) activity and the intracellular concentration of Ca^{2+}.

Additionally, A1 receptors couple to G_0, leading to an increased outward efflux of K^+ ions and a consequential stabilization of the neuronal membrane potential (see Figure 3). Moreover, activation of extracellular signal regulated kinase 1,2 (ERK1,2) and activation of PLD are induced by A3R stimulation. A3Rs undergo rapid desensitization through phosphorylation after exposure to an agonist, which is characterized by a loss of responsiveness and subsequent internalization. [4]

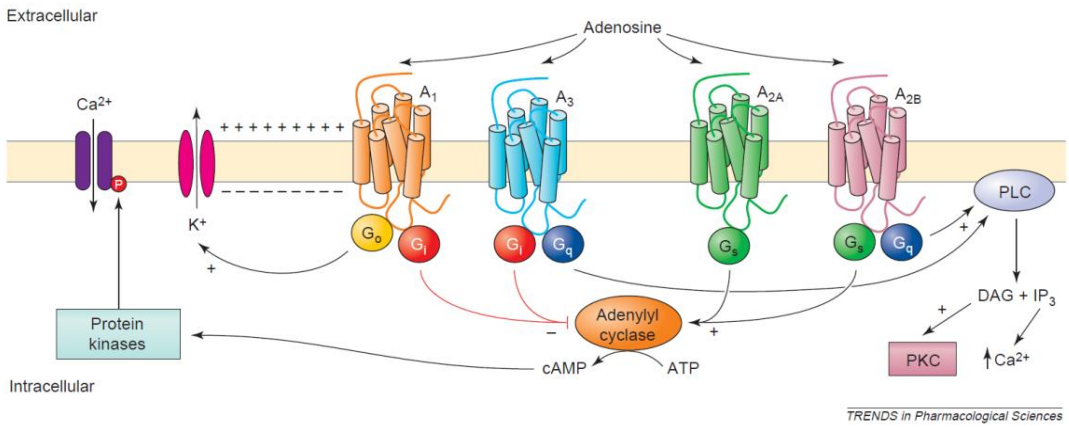

Figure 3: Signal transduction pathways associated with the activation of the human ARs. [4]

The adenosine receptors are involved in many pathophysiological processes in the human body and therefore display high potential as therapeutic targets. Selective adenosine receptor ligands are promising candidates for numerous therapeutic applications, both in the central nervous system (CNS) and in the periphery, including cardiovascular, inflammatory and neurodegenerative diseases (an overview is shown in Figure 4). [5]

1.1.1.1. A1R

The A1R plays various roles in the cardiovascular system: A1R activation causes a reduction of the heart rate and atrial contractility, attenuation of the stimulatory actions of catecholamines and displays a negative dromotropic effect on the AV-node. Intravenous administration of adenosine is indicated for arrhythmias, such as paroxysmal

supraventricular tachycardia (PSVT), to restore normal heart rhythm. Moreover, pharmacological data indicates that A1Rs play a role in the protection of the heart and brain from ischemia-reperfusion injury. [5]

In the central nervous system, A1R activation by adenosine leads to a global inhibitory modulation of synaptic transmission. There exists experimental evidence that adenosine exerts a neuroprotective effect in the event of acute ischemia, hypoxia and traumatic injury, which is mediated by the A1R. Moreover, adenosine, acting via A1 receptors, inhibits transmission of nociceptive inputs and therefore may be effective in decreasing postoperative and neuropathic pain in humans. [6]

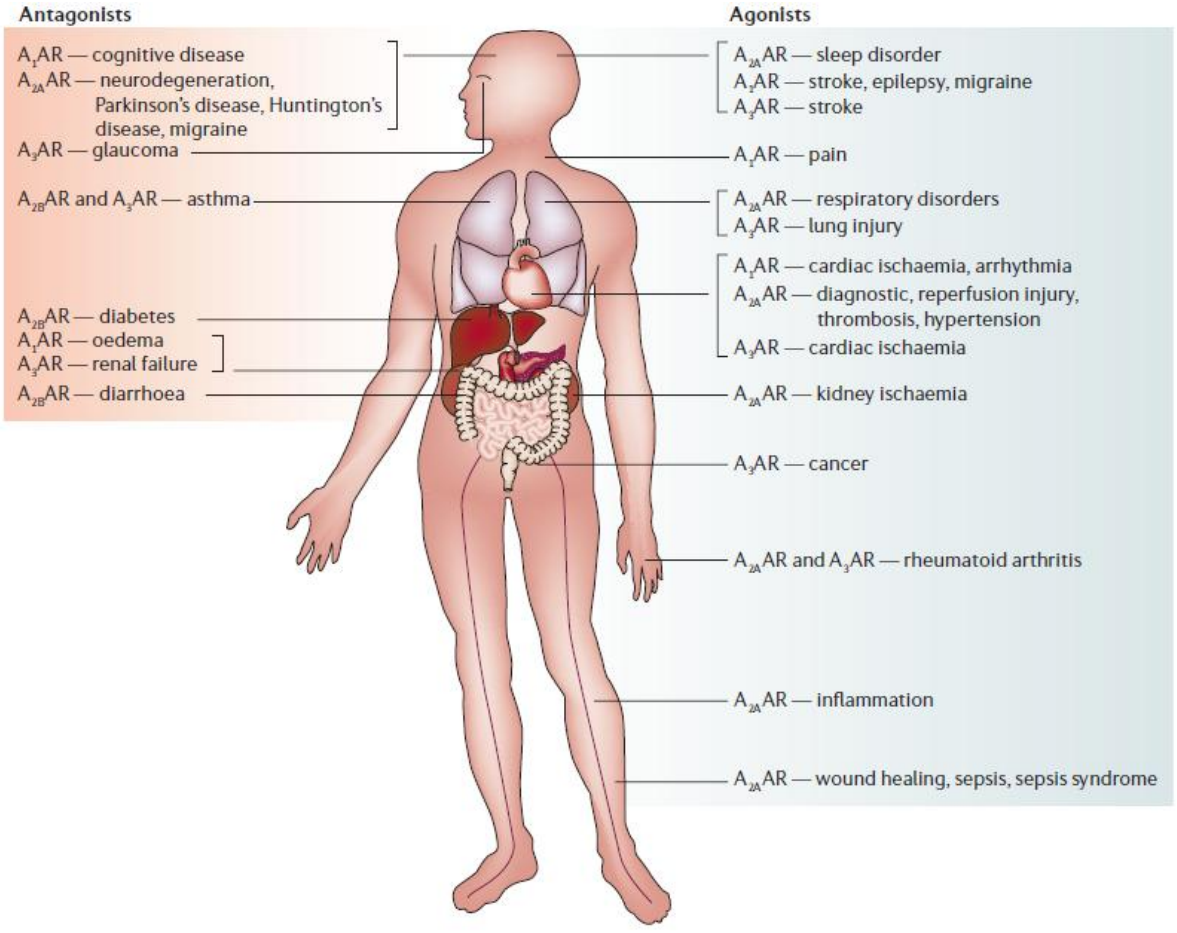

Figure 4: Novel disease targets for selective adenosine receptor ligands [5]

A1R activation leads to neuronal inhibition without concomitant vasoconstriction, indicating that this might be an effective treatment for migraine and cluster headache. In 2004, a novel

and selective A1R antagonist (FR194921), with the potential to treat dementia and anxiety disorders, was introduced. [5]

A1R agonists show a kidney protective effect and are considered for treating renal failure. In contrast, A1R antagonists are effective diuretic agents and are therefore useful in the treatment of fluid retention disorders. Moreover, a transgenic mice model, investigating obesity related insulin resistance, supports a significant physiological role for adipocyte A1R in the control of lipolysis. [5]

1.1.1.2. A2AR

The A2AR is present in blood vessels and mediates the vasodilator effect of adenosine in the brain and periphery. It is involved in vasodilatation in the aorta and coronary artery and therefore in regulating blood pressure. [5]

The A2AR is found in almost all immune cells including lymphocytes, monocytes, macrophages and dendritic cells. Through A2AR stimulation, adenosine inhibits T-cell activation and production of inflammatory cytokines while increasing the production of anti-inflammatory cytokines. Selective activation of the A2AR attenuates inflammation, reduces skin pressure and ulcer formation, and promotes wound healing. Due to those anti-inflammatory activity and wound healing effects, A2AR agonists are suitable for the treatment of chronic diabetic neuropathic foot ulcer. Because of the broad spectrum of anti-inflammatory activity observed in animal models, A2AR agonists are under consideration as therapeutic targets for asthma, sepsis and inflammatory bowel disease. [5]

A2AR activation was shown to promote myelination in Schwann cells, indicating the usability of selective agonists in the treatment of demyelinating diseases such as multiple sclerosis. [5]

Moreover, the A2AR plays a role in sleep regulation as it mediates the sleep-inducing effect of adenosine. The A2AR, which is antagonized by methylxanthines, is the primary mediator of the arousal and stimulatory effects of caffeine on the nervous system, like enhancement of awareness and learning. [5]

A neuroprotective effect of A2A receptor antagonists was observed in experimental models of ischemia, epilepsy, Parkinson´s disease and Huntington´s disease. Selective A2AR antagonists decelerate dopaminergic cell loss in patients with Parkinson´s disease and provide symptomatic improvement. There is epidemiological evidence that caffeine consumption reduces the risk of developing Parkinson´s disease by preventing degeneration of nigrostriatal dopaminergic neurons. [6]

1.1.1.3. A2BR

The A2BR mediates human chorionic vasoconstriction, inhibits cardiac fibroblast functions and stimulates nitric oxide production during Na^+ linked glucose or glutamine absorption. Stimulation of A2BR leads to angiogenesis by increasing the release of angiogenic factors. Unlike in mice, where mast-cell degranulation is mediated by the A3R, it is A2BR-dependent in humans. The bronchodilator and anti-asthmatic effects of theophylline and other xanthines might involve A2BR blockade, however the evidence is quite poor due to the lack of adequate animal models. [5]

1.1.1.4. A3R

The A3R plays an important role in protecting the heart, as overexpression leads to a decrease in heart rate, preservation of energetics and protection of the ischemic heart. Adenosine is released in large amounts during myocardial ischemia, resulting in effective preconditioning in cardiomyocytes through the activation of A3Rs. A3R mediated cardioprotection is achieved *in vivo* without entailing side effects such as hypotension or bradycardia and is therefore therapeutically more promising than A1R activation. [5]

Therefore, A3R agonists were suggested for the treatment of cerebral ischemia and rheumatoid arthritis. In addition to A1R agonists, A3R antagonists are suspected to have renal-protective properties. Furthermore, A3R antagonists were found to reduce intraocular pressure in mice and monkeys. Therefore A3R antagonists are potential candidate drugs for the treatment of glaucoma. The high expression level of the A3R in the lung suggests the use of A3R antagonists in treatment of asthma. [5]

1.1.2 The Role of Adenosine-3-Receptors in Cancer

The A3R is highly over expressed in various tumor cell lines: Madi et al. reported in 2004 that human melanoma, breast, colon, small-cell lung, and pancreatic carcinoma tissues express high levels of A3R-mRNA, whereas low expression was found in adjacent non-neoplastic tissue. Furthermore, they reported that lymph node metastasis expressed even more A3R mRNA than the primary tumor tissue, demonstrating a direct correlation between A3R expression and the degree of malignancy. [7]

In the same year, Gessi et al. analysed receptor binding values (K_d and Bmax) of the A3R ligand [^{3}H]MRE3008F20 in colorectal adenocarcinoma tissue samples. An increased A3R density was found in malignant tissue compared to healthy colon mucosa of the same individual. The authors reported that large adenomas showed increased binding, whereas small adenomas showed affinity and density values (K_d and Bmax respectively) that were similar to those of the mucosa of healthy subjects. This leads to the assumption that A3R levels may reflect the status of colorectal tumor progression and therefore disease severity. Another important result of the study indicates that the high receptor binding values were reflected in the peripheral blood cells of patients with colorectal carcinoma, since they found that peripheral lymphocytes and neutrophils from patients with colorectal cancer showed an overexpression of A3R compared to blood cells derived from healthy donors. [8]

Furthermore, it was shown by immunohistochemistry experiments, that primary thyroid cancer tissues express high levels of A3R versus normal thyroid tissue samples, which do not express the A3R. Moreover, up-regulation of A3R mRNA was found in hepatocellular carcinoma (HCC) tissues compared to adjacent normal tissues. Remarkably, A3R overexpression was also noted in peripheral blood mononuclear cells (PBMCs) derived from the patients with HCC, reflecting receptor status of the remote tumor tissue. [9] High expression levels of A3R in tumor tissues were directly correlated to elevated levels of NF-κB, which acts as an A3R gene transcription factor. [10]

"Taken together, the findings described above show that A3R over expression in different tumor cell types provide the rationale that this receptor may be utilized as a specific target to treat cancer." [9], as stated by Gessi S et al. (2008).

The A3R plays an important role in the regulation of the cell cycle, inducing either pro- or anti-apoptotic effects, depending on the level of receptor activation. Moreover, the A3R is involved in the regulation of cell growth, exerting a differential effect on tumor and normal cell proliferation. [9]

Upon treatment with synthetic A3R agonists (IB-MECA, Cl-IB-MECA and thio-Cl-IB-MECA) development and growth of leukemia, lymphoma, melanoma, colon, lung, breast and prostate carcinoma was suppressed *in vitro*. [11] IB-MECA and Cl-IB-MECA were tested both *in vitro* and *in vivo* at low concentrations and dosages. The agonists induced a cytostatic effect on tumor cells, manifesting in cell cycle arrest in G0/G1 phase. This effect was abolished by A3R antagonists, demonstrating that tumor growth inhibition was A3R mediated. [9]

Interestingly, for cordycepin (3´-deoxyadenosine), which is an active ingredient of a parasitic fungus (Cordyceps sinensis) used in traditional Chinese medicine, a remarkably anti-tumor effect on mouse melanoma and lung carcinoma cells was reported at micromolar concentrations. The inhibitory effect was blocked by the A3R antagonist MRS1191, demonstrating that the effect involves A3R stimulation. [9]

The anti-cancer effect of A3R agonists results from down-regulation of cyclin D1 and c-Myc, leading to cell cycle arrest and apoptosis of cancer cells. The underlying molecular mechanism involves the deregulation of signaling pathways related to Wnt and the nuclear factor kappa B (NF-κB). Upon A3R activation, cAMP levels decrease, resulting in a down-regulation of protein kinase A (PKA) and therefore decrease in protein kinase B (PKB/Akt), as it is phosphorylated by PKA. Consequently, this leads to an inhibition of IκB kinase (IKK) and subsequent accumulation of IκB/NF-κB complex in the cytoplasm. NF-κB is known to control the transcription of cyclin D1 and c-Myc, which play a crucial role in cell cycle progression. [10]

PKA and PKB/Akt also phosphorylate another signal protein, glycogen synthase kinase (GSK)-3β, representing a key modulator of the Wnt pathway. GSK-3β is crucial for β-catenin phosphorylation. After translocation to the nucleus, β-catenin induces again the transcription of c-Myc and cyclin D1, which are fundamental for cell cycle progression as already mentioned. Exposure of tumor cells to A3R agonists resulted in increased GSK-3β levels, as a result of PKA and PKB/Akt down-regulation, and subsequent phosphorylation and

ubiquination of β-catenin. This chain of events also leads to tumor growth inhibition by suppression of c-Myc and cyclin D. [10]

However, IB-MECA and Cl-IB-MECA administered at micromolar concentrations induce apoptosis and tumor cell growth inhibition through an A3R-independent mechanism, as the inhibitory effect was not abolished by antagonism or knockdown of the A3R. In 2003 it has been reported that IB-MECA down-regulates, at micromolar doses, the estrogen receptor alpha (ER-α) and suppresses human breast cancer cell proliferation. Obviously, at these relatively high concentrations, A3R agonists may interact with other receptors unspecifically, which may lead to a loss of selectivity. [9]

On the other hand, in normal cells A3R agonists induce the production of granulocyte-colony stimulating factor (G-CSF) by up-regulating the NF-κB signaling pathway. *In vivo* experiments confirmed an increase in white blood cells, when adenosine was administered before chemotherapy. [9]

Additionally, it has been observed that Cl-IB-MECA enhances activity of natural killer (NK) cells in naïve and tumor bearing mice by increasing IL-12 production through cAMP inhibition. IL-12 as a cytotoxic factor exerts a potent anti-tumor effect *in vivo* and therefore, A3R activation may contribute to NK cell-mediated destruction of tumor cells. [9]

Furthermore, the involvement of the A3R in hypoxic conditions, which are typical of solid tumors, has been investigated. The hypoxia inducible factor 1 (HIF-1) is one of the most important factors involved in cellular response to hypoxia and is found to be up-regulated in various cancer types. Its involvement in key aspects of tumor biology, such as angiogenesis, invasion, and altered energy metabolism, indicates a main contribution of HIF-1 to tumor progression and metastasis. Adenosine up-regulates HIF-1 protein expression in response to hypoxia in human melanoma, glioblastoma and colon cancer cells. Moreover, the A3R induces the expression of the vascular endothelial growth factor (VEGF) and angiopoietin-2, which in turn contributes to angiogenesis. Antagonism of A3R by appropriate ligands blocks HIF-1 as well as angiopoietin-2 and VEGF, leading once more to the assumption that A3R antagonists indicate a new approach for the treatment of cancer. [9]

1.1.3 THE A3R BINDING CAVITY

In January 2005, Stefano Moro and coworkers revisited the hypothetical binding site of the A3 receptor antagonists they had already proposed, using a rhodopsin-based homology modeling approach and site directed mutagenesis analysis. [4]

The A3 receptor model comprises of a seven-helix bundle with a central cavity, surrounded by helices 1-7 and 5-6, which is accessible from the cytosol, but not from the periplasm due to the hairpin (EL2) between TM4 and TM5 (see Figure 5a). This hairpin is located almost parallel to the membrane surface and has contacts with side-chains of most helices, like a disulfide bridge to TM3. Ligand recognition is supposed to appear in the upper region of the helical bundle, more precisely, TM3, TM5, TM6 and TM7 seem to be essential for ligand recognition (both agonists and antagonists). [4]

There have been several amino acid residues of the human A3 receptor within TM3, TM6 and EL2 mutated, which were assumed to contribute to ligand recognition, including His95, Trp243, Leu244, Ser247, Asn250 and Lys152. Following findings were obtained: "*The N250A mutation resulted in the loss of ability of the receptor to bind both radiolabeled agonist and antagonist whereas the H95A mutation significantly reduced the affinity of both agonists and antagonists for the receptor. By contrast, the K152A (EL2), W243A (TM6) and W243F (TM6) mutations did not significantly affect agonist binding but slightly decreased antagonist affinity, suggesting that these residues were crucial for the high affinity of human A3 receptor antagonists."* [4]

Moreover, they investigated the structure activity relationship (SAR) and proposed a novel Y-shaped 3D-pharmacophore model, which fits chemically and structurally to the molecular surface of the antagonist binding cavity (as shown in Figure 5b). The consensus binding motif comprises a set of structural features, which are directly related to the recognition of the ligand at the receptor site. The pharmacophore model occupies the upper region of the helical bundle, wherein the amino acids His95 (TM3) and Ser247 (TM6) appear to be essential for the recognition of antagonist structures. Remarkably, unlike the A1R and A2AR, the A3R lacks the histidine residue in TM6 that is common to the other subtypes (His251 in hA1R and His250 in hA2AR). This histidine residue has been shown to be crucial for ligand

binding to the A2AR and is replaced with a serine residue (Ser247 in hA3R). The asparagine residue Asn250, which is maintained by all adenosine receptor subtypes, enables a strong hydrogen bonding interaction and is significantly involved in ligand binding. Another feature of the proposed binding site model is a hydrophobic pocket characterized by non-polar amino acids, including Leu90 (TM3), Leu246 (TM6) and Ile (TM7). A further crucial pharmacophore region is located between Phe168 (EL2) and Phe182 (TM5) and is probably stabilized by π-π- interactions. Another important feature is a mostly hydrophobic region formed by three non- polar amino acids (Ile98 (TM3), Ile186 (TM5), Leu244 (TM6)). [4]

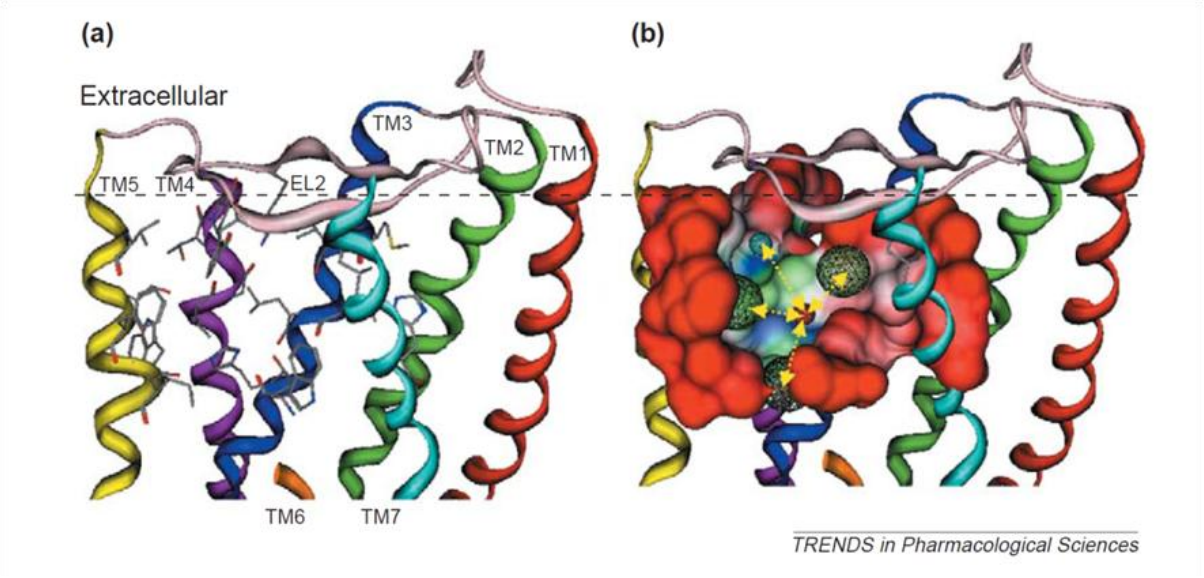

Figure 5: (a) General topology of the hA3R obtained using rhodopsin-based homology modelling (b) molecular surface of the transmembrane antagonist binding cavity and representation of the new proposed A3 receptor based pharmacophore model [4]

1.1.4 A3R ANTAGONISTS

The A3 receptor is the most recently discovered adenosine receptor subtype (Zhou et al, 1992). [12] In 1993, Salvatore et al successfully cloned the human adenosine-3-receptor. [13] It was demonstrated that the hA3R is distinct from the other subtypes, as there is little primary amino acid sequence identity: 50%, 43% and 40% to A1R, A2AR and A2BR, respectively.[14] Moreover, the A3R shows large interspecies differences, regarding homology sequences, pharmacological profile and peripheral distribution. Affinity of antagonists for A3 receptors of rats and humans can differentiate dramatically, pointing at the low identity (72%) of protein sequences between hA3R and rA3R. [14]

As a main approach to discovering and developing AR agonists, adenosine itself was modified, including N6-substitution and modification of the 5´-position. This led, for example, to the development of CPA (K_i=2.3nM for hA1R), IB-MECA (K_i=1.8nM for hA3R) and CGS21680 (K_i=27nM for hA2AR). [5] In case of AR antagonists, xanthines such as caffeine and theophylline were modified, leading to the classical antagonists of A1R, A2AR and A2BR (e.g. DPCPX K_i=3.9nM for hA1AR). The search for A3R antagonists began with the discouraging observation that xanthines only have intermediate affinity for the human A3R (typically 100nM for 8-phenylxanthine analogues). Thus, the focus turned towards novel heterocyclic systems, making screening of diverse chemical libraries necessary to identify novel leads for the human A3R, such as 1,4-dihydropyridines, flavonoids, pyridines, thiazoles and others. [5]

Jacobson and coworkers thoroughly examined the 1,4-dihydropyridine scaffold as a template for investigating the structure activity relationship at the A3R. Different substitutions and modifications of groups were probed at 4- and 5-positions, including the enlargement of the substituent at position 4 and the ester at position 5. Both led to the enhancement of A3R affinity and selectivity towards L-type calcium channels, which are known targets of 1,4-dihydropyridines. [14] Especially, the phenylethynyl group at the position 4 and benzylester at 5-position (MRS1191, K_i=31.4nM) was beneficial to both affinity and selectivity at hA3R (see Figure 6 for chemical structure). [15]

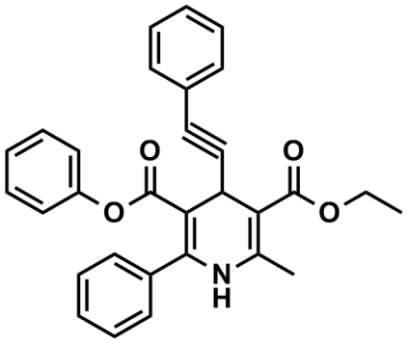

Figure 6: Chemical structure of MRS1191

Moreover, they studied the affinity of pyridines, derived from the oxidation of the corresponding 1,4-dihydropyridines, of which the most suffered the loss of affinity and selectivity towards the hA3R with a few exceptions. Remarkably, bulky substituents in 4-position, which are beneficial regarding the affinity of 1,4-dihydropyridines, are not well tolerated within the pyridines. This observation is explainable by the change in the C5-C4-R4 angle from 68.1° to 0.2° due to the change in C4-hybridization. For that reason, small alkyl groups at the 4-position of the pyridines are essential to maintain affinity and selectivity towards the hA3R. [14] Ethyl and propyl are suitable substituents at 4-position as it was shown for FE@SUPPY (K_i=4.22nM (hA3R), see Figure 8 for chemical structure) [16] and MRS1523 (K_i=18.9nM (hA3R), see Figure 7 for chemical structure) [17], respectively.

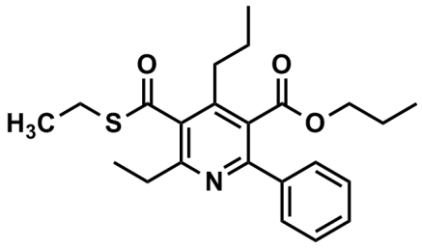

Figure 7: Chemical structure of MRS1523

In 1998, Li et al reported that 3,5-diacyl-2,4-dialkyl-6-phenylpyridine derivatives have been found to be potent and selective antagonists at both human and rat A3 adenosine receptors. The authors synthesized novel 3,5-diacylpyridines derivatives by introducing various

functional groups and they intensively probed structure-activity relationships at various positions of the pyridine ring, including 3- and 5-acyl substituents and the 2- and 4-alkyl substituents. The tetraethyl analogue, MRS1476, which was considered hitherto one of the most potent compounds at the hA3R (K_i=20.0nM±1.9), was substituted with a β-flourethylester at the 5-position of the pyridine resulting in a 5-fold enhancement of affinity at hA3R (K_i=4.22nM±0.66). [16] This compound was later named FE@SUPPY by our working group (Figure 8). [18]

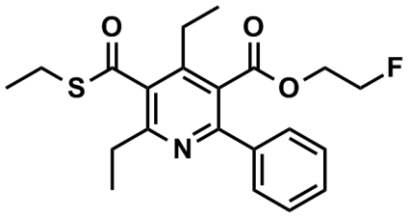

Figure 8: Chemical structure of FE@SUPPY

Substitution with a γ-fluoropropylester was also beneficial to the affinity at hA3R (K_i=9.67nM±3.34), but not the pentafluoropropyl analogue (K_i=446nM±119), which was significantly less potent. Introducing steric bulky groups at the 4-position (phthaloylamino analogues) resulted in less potent compounds at the A3R. Increased human A3R affinity was observed for the 5-propylester, but not for the 4-propyl analogue, however a disadvantage of the 5-propylester derivative was the relatively high affinity at the rat A3R, which in turn favors the 4-propyl derivative. The ethyl group in 2-position was modified in the form of β-hydroxyethyl leading to a decline in affinity at hA3R, while the β-fluoroethyl group at the same position greatly increased affinity. Substitution with both acetylthioethyl and benzyloxyethyl in 2-position led to K_i values > 100nM. Replacing the 3-ethylthio ester by a β-hydroxyethylthio ester resulted in a 3-fold less potent compound than the corresponding. Moreover, fluoro substitution of the 6-phenyl group at ortho, meta and para positions did not show significant benefit. Concluding, the two fluoro derivatives mentioned above (K_i value of 4.22nM and 9.67nM, respectively) are the most potent pyridines as the results prove. The attempt to improve water solubility by introducing hydroxyl groups while increasing A3R affinity failed. [16]

1.1.5 PROJECT BACKGROUND

There is a rising scientific interest in the field of A3R research, as this receptor is involved in various pathologies as cancer, asthma, inflammation and neurodegeneration (see 1.1.1.4). A PET-tracer for the A3R would represent a key advance towards the characterization of the hA3R *in vivo*, elucidating the function of this relative unexplored receptor in the human body. Moreover, an A3R PET-tracer would open new perspectives in the field of molecular imaging of tumor related pathologies. [^{18}F]FE@SUPPY, the first PET ligand for the adenosine A_3 receptor was introduced in 2008. [18],[19] The radiochemical preparation of both tracers, [^{18}F]FE@SUPPY and [^{18}F]FE@SUPPY:2, was automated successfully. [20] So far, preclinical evaluation including autoradiography, biodistribution, logP was conducted. The assessment of the *in vitro* and *in vivo* stability was investigated in metabolite studies. [21] This project was sponsored by the Austrian Science Fund (FWF P19383-B09) awarded to M. Mitterhauser.

1.2 Radioligand Binding Assays

1.2.1. Principles of Competition Assays

Radioligand binding assays are used to examine and quantify the interaction between a ligand and its receptor. Most analysis of binding experiments (determination of binding parameters) are based on the law of mass action, a model describing the formation of a ligand-receptor complex, assuming a reversible binding (see Figure 9). [22]

$$\text{Ligand} + \text{Receptor} \leftrightarrow [\text{Ligand} \cdot \text{Receptor}]$$

Figure 9: law of mass action [23]

According to the law of mass action, association and simultaneous dissociation events take place until equilibrium is reached. At equilibrium, the rate at which new ligand-receptor-complexes are formed equals the rate at which complexes dissociate (see Figure 10). [22]

$$[\text{Ligand}] \cdot [\text{Receptor}] \cdot k_{on} = [\text{Ligand} \cdot \text{Receptor}] \cdot k_{off}$$

Figure 10: k_{on} association rate constant, k_{off} dissociation rate constant [23]

$$\frac{[\text{Ligand}] \cdot [\text{Receptor}]}{[\text{Ligand} \cdot \text{Receptor}]} = \frac{k_{off}}{k_{on}} = K_d$$

Figure 11: Definition of equilibrium dissociation constant K_d [23]

The equilibrium dissociation constant K_d (Figure 11) is the main parameter specifying the affinity of an agonist for a receptor. It is a measure of the strength of the interaction of a ligand to its receptor. Per definition, the K_d is the concentration of the ligand which occupies

half of the receptors, which means that agonists with small K_d values have a high affinity for a receptor. [24] K_d values are usually determined in saturation binding assays. [23]

Analogically, the inhibition constant (K_i) specifies the binding affinity of an inhibitor for a receptor. For the investigation of K_i values of unknown (unexplored) compounds, competition-binding-assays are very useful tools, providing that a radiolabeled agonist (K_d already determined) is available. Preparations of membranes, expressing the target receptor, are incubated with a constant concentration of radioligand and varying concentrations of test-compound (inhibitor). Unlabeled compounds are tested in a wider range of concentrations (e.g. 0,1nM–1µM) to compete the binding of a fixed concentration of a radioligand. [25]

Competitive binding curves are obtained by plotting specific binding (Y axis) against the logarithm concentration of the competitive inhibitor (X axis). Specific binding is expressed as the difference between top (total binding) and bottom (non-specific binding) plateaus of the curve (Figure 12). [24]

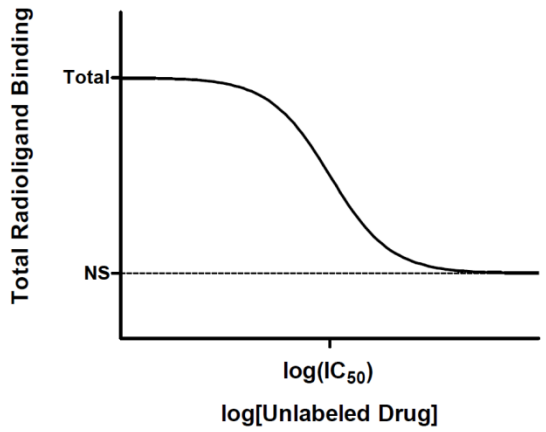

Figure 12: Competitive binding curve [26]

Total binding reflects radioligand binding in the absence of the competing inhibitor, which equals 100% binding. Considering that radiolabeled compounds bind in an extent to surfaces (biological and synthetic materials) in an unspecific manner, nonspecific binding has to be determined by blocking all receptors with a potent competitor (agonist or antagonist). For

these purposes membrane preparation and radioligand are incubated with high concentration of competitor (about 1000-fold its K_d). [24]

Generally, nonlinear regression is used to fit the corresponding curves. The point of inflection of the competitive binding curve corresponds to the IC_{50} (inhibitory concentration 50%), which is the concentration of unlabeled compound that blocks half the specific binding of radioligand. For calculating the K_i, the equation of Cheng and Prusoff is used (see Figure 13). [27]

$$K_i = \frac{IC50}{1 + \frac{[RL]}{K_d}}$$

Figure 13: The Cheng & Prusoff equation. IC_{50} is the concentration of test substance that blocks half the specific binding of the radioligand, [RL] is the concentration of used radioligand and K_d is the affinity value of the radioligand [27]

1.2.2 Receptor Binding Assays: Techniques

Receptor binding assays are very useful as a screening procedure for new ligands regarding their affinity (determination of K_d or K_i values). They allow a plurality of samples to be processed with time-saving operation (i.e. semi-automated method). Receptor binding assays may be conducted using intact cells (isolated whole cell preparations) as well as membrane preparations and soluble receptors. [28] During this thesis, membrane preparations were used since cells are lysed and there are no other cellular components within the preparations. Furthermore, these membrane preparations are commercially available which assured high quality and reduced time and operational burden of cell culture methods.

The basic principle of a receptor binding assay using membrane preparations involves

1) radioligand incubation

2) separation of bound and free radioligand and

3) detection of radioactivity. [28]

In the following these three points are explained in more detail.

Ad 1) During incubation, the radioligand binds to the target receptor (in the absence or presence of a displacing agent), allowing an equilibrium to be reached between bound and free ligand. There are many variables within this incubation as the used buffer, time, temperature and volume that have to be investigated when setting up new assays. Ionic strength, ion composition and the pH values of the used buffer are essential parameters as well, as stated by Qume M: *"… changes in pH may have effects on the ionization of groups within the receptor or on the ligand, affecting receptor ligand interactions, influencing both the equilibrium binding constant and the kinetic rate constants"* [28]. The addition of enzyme inhibitors (such as adenosine deaminase) or chelating agents (such as EDTA) to the buffer can be useful; however there is evidence that they may affect ligand binding: *"To reduce the presence of endogenous ligand, enzymes such as adenosine deaminase may be included in the buffer, although care should be taken to ensure that the radioligand used is not subject to metabolism by the enzyme".*[28] Performing the assay at low incubation temperature

reduces degradation of ligand and/or receptor, but in turn increases the incubation time required to reach binding equilibrium. Moreover, the lower the radioligand concentration applied, the longer it will take until equilibrium occurs. [28]

Ad 2) Incubation is followed by termination of the reaction by separating the receptor-ligand-complex from free radioligand, what can be conducted by filtration or centrifugation. When using centrifugation, the bound ligand remains with the particulate matter in the resulting pellet. Free ligand, contained in the supernatant, has to be tipped out or aspirated off. Followed by rewashing the pellet to remove any free ligand remaining, requiring manually handling, what in turn scales down the number of samples in one batch. In contrast, when using filtration, the ligand-receptor-complex remains on the filter, which is then rewashed to remove free ligand. Subsequently radioactivity present on the filter can be determined (see Ad 3)). Samples can be filtered by hand or alternatively, by using a commercial available filtration system (e.g. Brandel® Cell Harvester), that efficiently filters and washes many samples at the same time, reducing variability. [28]

Cell Harvesters are semi-automated vacuum filtration systems (see Figure 14), providing simultaneously aspiration and uniform washing of cells. The hot-cold wash valve provides the separate collection of radioactive and nonradioactive waste material, making waste disposal economical. Cell Harvesters are easily manageable and the filtration method is less time consuming. [29] Therefore, we decided in favor of the filtration method using a cell harvester.

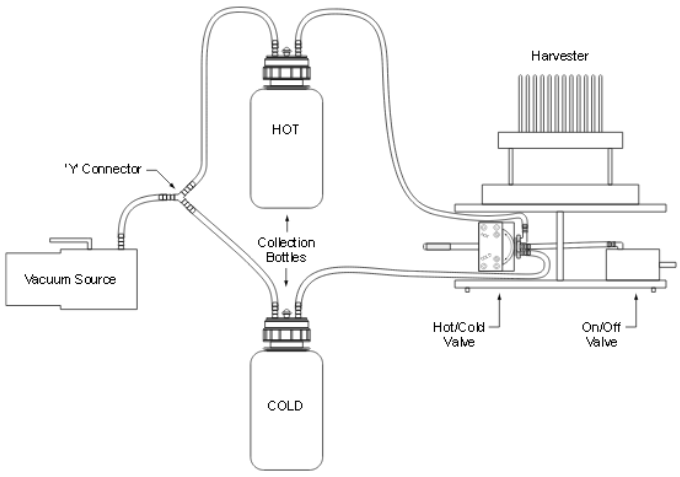

Figure 14: Scheme of the Brandel® Cell Harvester System [29]

Washing is also a crucial step, as it helps to get rid of unbound ligand and therefore reduces nonspecific binding. Insufficient washing may lead to overestimating the bound fraction. Whereas, increasing the number of washing steps or the volume of wash buffer may cause dissociation of the bound ligand and therefore underestimation. Ice-cooling the wash buffer prior to use reduces dissociation. Nonspecific binding comes about through free radioligand insufficiently washed off as well as through radioligand binding nonspecifically to any sites of the filter. High levels of nonspecific binding may lead to difficulties in samples with low specific binding of radioligand. Thus, the assessment of nonspecific binding is very essential. Pretreatment of filters with antiadsorbants (i.e. 0,1-0,5% polyethylenimine, bovine serum albumine) may reduce nonspecific binding to an acceptable level. [28] *"Treating filter plates with polyethylenimine is a common practice to minimize ligand binding to filters. PEI is a cationic polymer that can neutralize the negative charge of the glass fiber filter."* [30]

Ad 3) After filtration, single circular shaped filters derived from each probe are counted. Gamma emitters such as ^{125}I allow direct quantification of the radioactive content of the filter, whereas beta emitters require the addition of a scintillating fluid. The energy emitted from tritiated ligands is converted into photons by the scintillator, which can then be detected by fluid scintillation counting. [28] The determination of radioactivity is used to quantify the radioligand that has bound to the receptor. Competitive binding curves allow the determination of the IC50 value and subsequently of the affinity value (K_i) of the competitor via the Cheng&Prusoff equation (Figure 13 in 1.2.1). For analysis of data see 3.3.7.

2 AIM

The A3R is a potential target for molecular imaging of tumor-related pathologies, due to its overexpression in primary and metastatic tumors (human melanoma, colon, breast, small-cell lung cancer, pancreatic carcinoma tissues and lymph node metastasis) versus low expression in non-neoplastic tissue. Hence, aim of this work was the determination and evaluation of a ligand with high affinity and selectivity as a potential new PET-tracer for the A3R.

Therefore, several new FE@SUPPY-derivatives, as well as the well-established A3R antagonists FE@SUPPY and FE@SUPPY:2, were evaluated regarding their affinities towards the human adenosine receptor subtypes A1R, A2AR and A3R using the cell-harvester method. Binding profiles were compared with pharmacologically known and evaluated compounds as proof of concept for all receptor assays. In case of the A3R, the antagonists MRS1191 and MRS1523 were used as model compounds.

In detail, the newly synthesized FE@SUPPY-derivatives FE@SUPPY:11, FEMe@SUPPY:2, FE^2@SUPPY, Me^2@SUPPY were tested for their respective affinities for the hA1R, hA2AR and hA3R. Optimal candidates for imaging the A3R should display high affinity (K_i<10nM) for the A3R, and low affinity (K_i≥1µM) for the other subtypes.

Moreover, the binding profile of DFE@SUPPY and DFE@SUPPY:2, the respective metabolites of the PET-tracers [^{18}F]FE@SUPPY and [^{18}F]FE@SUPPY:2, were investigated. In addition, structurally related ligands as FE@CAPPY, Me^2@CAPPY, and structurally different ligands as BD1 and BD3, were in the scope of the study.

Apart from that, we aimed to optimize radioligand binding assays in order to receive reproducible and reliable data and establish the filtration method using a Brandel® Cell Harvester in our laboratory.

3 MATERIALS AND METHODS

3.1 MATERIALS

Radiolabeled compounds [^{125}I]AB-MECA (NEX312), [^{3}H]CGS12680 (NET1021), [^{3}H]DPCPX (NET974) and Membrane Target Systems™ (hA2AR (RBHA2AM400UA), hA1R (ES-010-M400UA) and hA3R (ES-012-M400UA)) were purchased from PerkinElmer® (Waltham, USA). CGS21680, I-AB-MECA, MRS1523 and MRS1191 were obtained from Sigma- Aldrich® (St. Luis, USA). DPCPX and SCH442416 were purchased from Tocris Bioscience (Bristol, UK). BD1, BD3, DFE@SUPPY, DFE@SUPPY:2, FE@CAPPY, FE@SUPPY, FE@SUPPY:2, FE@SUPPY:11, FEMe@SUPPY:2, FE^{2}@SUPPY, Me^{2}@CAPPY and Me^{2}@SUPPY were synthesized by the Department of Natural Drug Synthesis, University of Vienna (provided by Prof. Dr. Helmut Spreitzer). Chemical structures and IUPAC names of the ligands are shown in Table 1.

Adenosine deaminase (ADA), bovine serum albumin (BSA), dimethylsulfoxide (DMSO), ethylenediaminetetraacetic acid (EDTA) disodium salt dihydrate, sodium chloride, tris(hydroxymethyl)aminomethane (Tris), and (N-[2-hydroxyethyl])-piperazine-N`-[2-ethanesulfonic acid]) (Hepes), Polyethyleneimine (PEI, 50% (w/v) in H_2O) were purchased from Sigma- Aldrich® (St. Luis, USA). Magnesium chloride was obtained from Merck (Darmstadt, Germany). Ultima Gold™ (high flash point LSC cocktail, biodegradable) was purchased from PerkinElmer® (Waltham, USA). Test tubes (5ml, 75x12mm, polypropylene) and scintillation vials (20ml, polypropylene) were purchased from Sarstedt (Nümbrecht, Germany). Snap Cap Bio- Vials™ were purchased from Beckman Coulter GmbH (Monheim, Germany).

BD1	N,N-dimethyl-2-((1-methyl-6-phenyl-1,6-dihydropyrazolo[3,4-e]indazol-4-yl)oxy)ethanamine	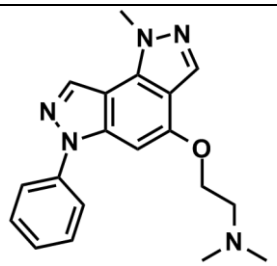
BD3	1-methyl-4-(2-(4-methylpiperazin-1-yl)ethoxy)-6-phenyl-1,6-dihydropyrazolo[3,4-e]indazole	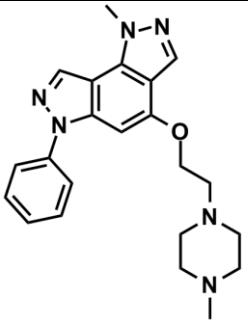
CGS21680	3-(4-(2-((6-amino-9-((2R,5S)-5-(ethylcarbamoyl)-3,4-dihydroxytetrahydrofuran-2-yl)-9H-purin-2-yl)amino)ethyl)phenyl)propanoic acid	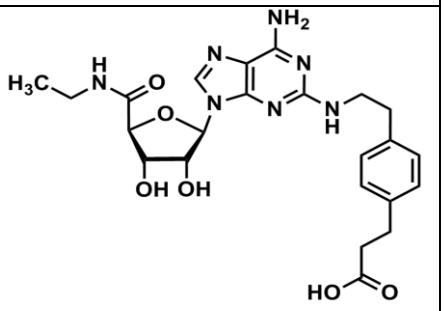
DFE@SUPPY	4,6-diethyl-5-((ethylthio)carbonyl)-2-phenylnicotinic acid	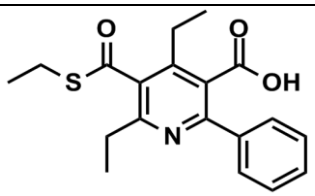
DFE@SUPPY:2	5-(ethoxycarbonyl)-2,4-diethyl-6-phenylpyridine-3-carbothioic S-acid	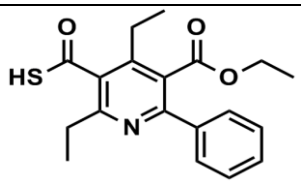
DPCPX	8-cyclopentyl-1,3-dipropyl-1H-purine-2,6(3H,7H)-dione	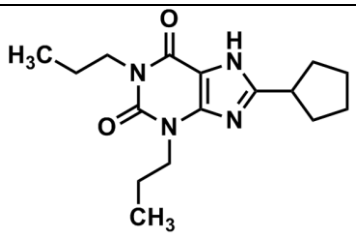

FE^2@SUPPY	2-fluoroethyl 4,6-diethyl-5-(((2-fluoroethyl)thio)carbonyl)-2-phenylnicotinate	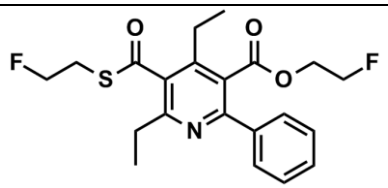
FE@CAPPY	3-ethyl 5-(2-fluoroethyl) 2,4-diethyl-6-phenylpyridine-3,5-dicarboxylate	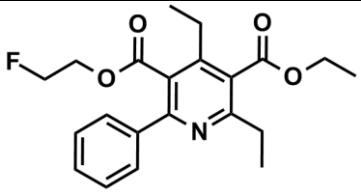
FE@SUPPY	2-fluoroethyl 4,6-diethyl-5-((ethylthio)carbonyl)-2-phenylnicotinate	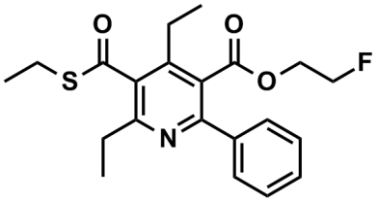
FE@SUPPY:2	ethyl 4,6-diethyl-5-(((2-fluoroethyl)thio)carbonyl)-2-phenylnicotinate	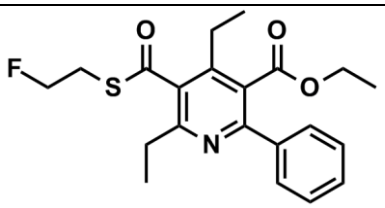
FE@SUPPY:11	2,4-diethyl-5-((2-fluoroethoxy)carbonyl)-6-phenylpyridine-3-carbothioic S-acid	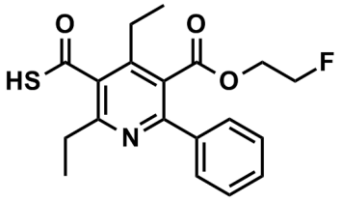
FEMe@SUPPY:2	methyl 4,6-diethyl-5-(((2-fluoroethyl)thio)carbonyl)-2-phenylnicotinate	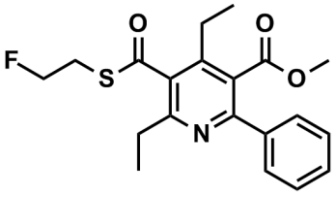
I-AB-MECA	(5R)-5-(6-((4-amino-3-iodobenzyl)amino)-9H-purin-9-yl)-3,4-dihydroxy-N-methyltetrahydrofuran-2-carboxamide	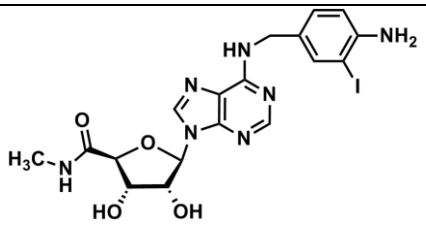

Me^2@CAPPY	dimethyl 2,4-diethyl-6-phenylpyridine-3,5-dicarboxylate	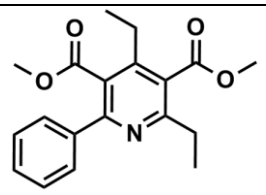
Me^2@SUPPY	methyl 4,6-diethyl-5-((methylthio)carbonyl)-2-phenylnicotinate	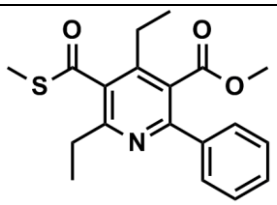
MRS1191	3-ethyl 5-phenyl 2-methyl-6-phenyl-4-(phenylethynyl)-1,4-dihydropyridine-3,5-dicarboxylate	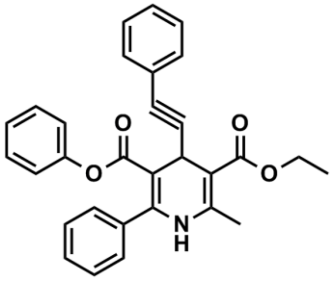
MRS1523	propyl 6-ethyl-5-((ethylthio)carbonyl)-2-phenyl-4-propylnicotinate	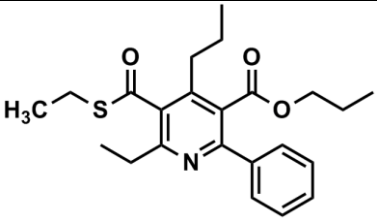

Table 1: Chemical structures and respective IUPAC names of the ligands used in competitive binding experiments

3.2. INSTRUMENTATION

Radioligand binding assays were performed with a M-36 tygon tubed Cell Harvester (Brandel®, Gaithersburg, USA) (see Figure 15) using Whatman™ GF/B Filters. Beta- Counting was conducted with a 300 SL Automatic TDCR Liquid Scintillation Counter (HIDEX, Finland). Ultima Gold™ (high flash point LSC cocktail, biodegradable) was purchased from PerkinElmer® (Waltham, USA). Gamma- Counting was done with a Wallac Wizard^2 3`` ™ purchased from PerkinElmer® (Waltham, USA). For Pipetting Eppendorf Reference® (variable 100-1000µl and 10-100µl) were used. Labinco® Vortex Mixer was used for homogenization.

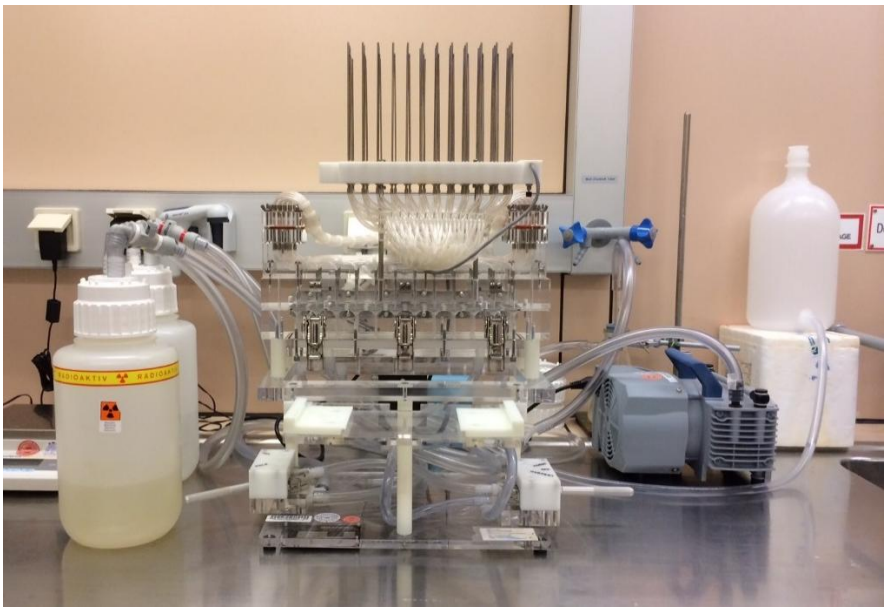

Figure 15: Brandel® Cell Harvester, Laboratory of Radiochemistry and Biomarker Development Unit, Medical University of Vienna, Austria

3.3 METHODS

3.3.1 PROPORTIONING AND DILUTION OF MEMBRANES

Proportioning of membranes expressing the human A1R was carried out as follows: The Lot of 400µl frozen membrane (protein concentration 10µg/µl) was thawed and split in 12 aliquots à 33,3µl, resulting in a protein concentration of 333µg protein per aliquot. Immediately after proportioning, aliquots were frozen again and stored at -80°C. For the assay one aliquot was resuspended in 3,6ml wash buffer, leading to a final protein concentration of 18,5ng/µl in 500µl total volume (9,25µg protein per vial). (For detail information about the product see Technical Data Sheet ES-010-M400UA, Appendix)

Membranes expressing the human A2AR (9µg/µl protein concentration) were prepared as described for the A1R assay, resulting in a protein concentration of 8,1µg in 500µl total volume (16,65ng/µl). (For detail information about the product see Technical Data Sheet RBHA2AM400UA, Appendix)

In case of membranes expressing the human A3R, 400µl of frozen membrane (protein concentration 1,5µg/µl) were divided in 20 aliquots à 20µl, implicating 30µg protein per aliquot. Aliquots were stored at -80°C. For the assay one aliquot was resuspended in 3,6ml wash buffer, leading to a final protein concentration of 1,67ng/µl in 500µl total volume (0,84µg protein per vial). (For detail information about the product see Technical Data Sheet ES-012-M400UA, Appendix)

3.3.2 DILUTION OF RADIOLIGANDS AND DECAY CORRECTION

The dilution to the desired concentration of the respective radioligands was conducted as follows:

In case of A1R binding assay, PerkinElmer® recommended a radioligand concentration of 1,7nM [^{3}H]Cyclopentyl-1,3-dipropylxanthine (see Appendix for Technical Data Sheet,

NET974). Therefore, 3,7µl [^{3}H]DPCPX (specific activity 4,44TBq/mmol) were taken and diluted in 1,8ml buffer (amount for 36 samples), receiving a 17nM dilution. 50µl of 17nM [^{3}H]DPCPX were added to each vial, leading to a final concentration of 1,7nM in 500µl total volume. See Figure 16 for calculation.

$$C = \frac{C_A}{A_S} = \frac{37\ \mathrm{MBq/ml} \times 1000}{4{,}44\ \mathrm{TBq/mmol}} = 8333{,}33\mathrm{pmol/ml} = 8333{,}33\mathrm{nM}$$

$$\frac{50\mu\mathrm{l} \times 17\mathrm{nM} \times 36}{8333{,}33\mathrm{nM}} = 3{,}672\mu\mathrm{l}$$

Figure 16: Calculation of desired volume [^{3}H]DPCPX via specific activity, C_A = activity concentration, A_S= specific activity (both stated in the Technical data sheet, Appendix)

A2AR competition experiments were performed with [^{3}H]CGS21680 (NET1021, see Appendix for Technical Data Sheet). Depending on the specific activity of the used batch (A_S= 1,302TBq/mmol Lot No 1735316, A_S= 1,334TBq/mmol Lot No 1651413) 31,7µl–32,4µl radioligand were diluted in 1,8ml wash buffer to achieve a final concentration of 50nM in total volume of assay probes.

In contrast to the tritium labeled ligands (half-life of 12,32 years), we had to consider radioactive decay regarding ^{125}I with a half-life of 59,41 days. Therefore a decay correction was conducted every two days in order to obtain the desired concentration of radioligand. For example, the decay 14 days after calibration of the batch was calculated as follows: The initial activity of a 0.5ml batch was 3.19MBq (Lot Nr. GU01830, NEX312). The desired final concentration of radioligand is 0.4nM which corresponds to a chemical amount of 7,2pmol. The remaining amount of radioactivity after 14 days ($N_{(t)}$, t= 14) was calculated with the equation of exponential decay (see Figure 17), yielding 2,71MBq.

$$N_{(t)} = N_{(0)} \times e^{-\lambda \times t}$$

$$\lambda = \frac{\ln(2)}{t_{1/2}}$$

$$3{,}19\text{MBq} \times e^{-\ln(2)/59{,}41\text{d} \times 14\text{d}} = 2{,}71\text{MBq}$$

Figure 17: Equation of exponential decay: $N_{(t)}$ is the quantity at time t, $N_{(0)}$ is the initial quantity, λ is the exponential decay constant and $t_{1/2}$ is the half-life [28]

Then the correction factor was determined (3,19/2,71=1,177) and the volume of radioligand, which has to be taken out of the batch was corrected by this factor (91,86µl × 1,177 = 108,16µl).

A3R competitive binding assays were performed with 50µl 4nM [^{125}I]AB- MECA, leading to a final concentration of 0,4nM in 500µl total volume. The required amount of [^{125}I]AB- MECA (C_A= 6,38MBq/ml, A_S= 81,4TBq/mmol) was more than 90µl. For financial and economic reasons, we decided to add unlabeled I-AB-MECA as a carrier.

3.3.3 Preparation of Stock Solutions and Dilution Series of Compounds

Stock solutions and standards of test compounds were prepared in DMSO. For further dilutions (dilution series), buffer or for poorly water-soluble compounds a mixture of buffer/DMSO was used. Considering that DMSO is toxic to cells and biological material, a maximum of 10-15% DMSO was tolerated within the assays.

Dilution series were made on the basis of a 1mM standard solution in DMSO (see Figure 18). Thus, 100µM dilutions of test compounds, which were generally used within A1R and A2AR assays, contained 10% DMSO in final volume of assay probes. Dilutions of test compound in concentrations ≤10µM were prepared with a content of maximum 1% DMSO. Within the A2AR assay, assay buffer, containing ADA, was used for diluting test compounds. Within the A1R assay, dilution of competitors was conducted with the respective A1R assay buffer (see 3.3.4 for exact composition of buffers).

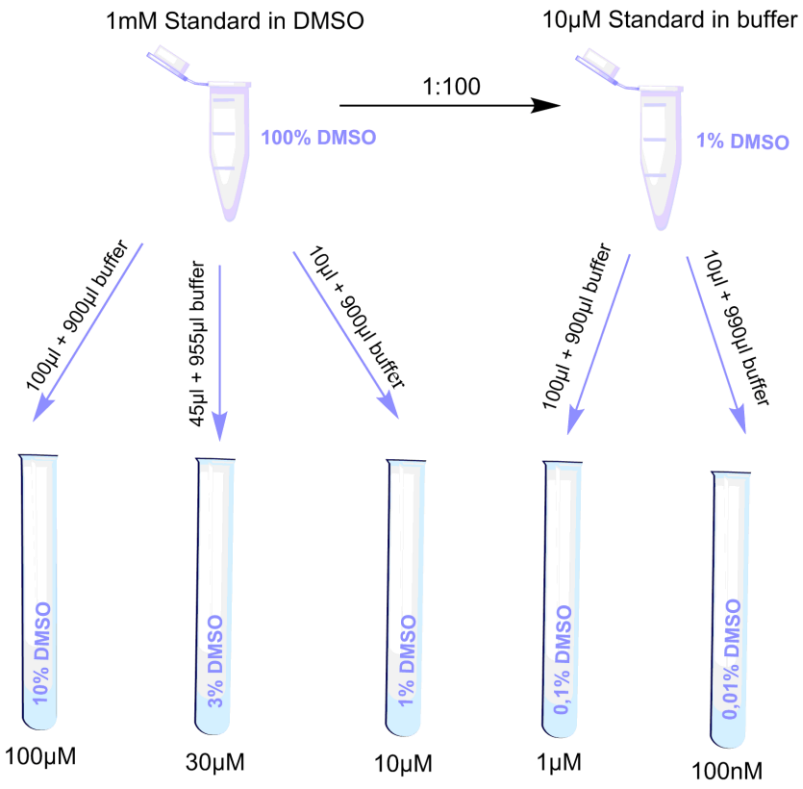

Figure 18: scheme of dilution series

Regarding the A3R assay, wash buffer, assay buffer or deionized water were used for dilution of test compounds and assay probes contained 0-10% DMSO depending on solubility of the test compound (solvents and content of DMSO is declared in the results section).

3.3.4 Composition of Buffers

A1 receptor assay

The buffer, used for diluting, aspirating and washing within the A1R assay, consisted of 25mM Hepes pH 7.4, 5mM $MgCl_2$, 1mM $CaCl_2$ and 100mM NaCl. Washing procedure was conducted with ice-cold buffer. For 1L buffer, 5.96g Hepes (MG= 238.3g/mol), 1.02g $MgCl_2$

(MG= 203.3g/mol), 0.15g $CaCl_2$ (MG= 147.02g/mol) and 5.84g NaCl (MG= 58.44g/mol) were solved in distilled water. PH was adjusted to 7.4 using NaOH.

A2A receptor assay

In case of the A2AR assay, two different buffers were used: the assay buffer (used for diluting membranes, radioligand and competitors as well as aspirating the probes) and the wash buffer (used for washing procedure). Assay buffer contained of 50mM Tris–HCl, 10mM $MgCl_2$ and 1mM EDTA. Adenosine deaminase was added (1ml/L) to degrade endogenous adenosine potentially present in the membrane preparation. Wash buffer (50mM Tris-HCl, 154mM NaCl) was used for rewashing the filter and was kept on ice prior to use.

A3 receptor assay

The assay buffer used for the A3R competitive binding experiments consisted of 25mM Hepes pH 7.4, 10mM $MgCl_2$, 1mM $CaCl_2$, and 0,5% BSA. An ice-cold Tris-HCl solution (50mM, pH 7.4) was used for the washing procedure.

3.3.5 Determination of Total and Nonspecific Binding

Total binding of radioligand ([^{125}I]AB- MECA, [^{3}H]CGS21680 and [^{3}H]DPCPX) was determined in the absence of competitor, incubating 100µl of the respective membrane preparation, 50µl radioligand and 350µl buffer instead of test compound.

Nonspecific binding of radioligand was determined in the presence of saturation concentrations of an unlabeled ligand with known K_d value. Therefore the unlabeled ligand was used in concentrations 100 to 1000-fold of its K_d value to ensure that all receptors were occupied by the ligand and consequently the radioligand only bound unspecifically.

More precisely, 1µM DPCPX (hA1R assay), 1µM SCH442416 (hA2AR assay) and 10µM I-AB-MECA (hA3R) were used to determine nonspecific binding of the respective radioligands.

3.3.6 IMPLEMENTATION OF THE ASSAY

Competitive binding experiments (hA1R, hA2AR, hA3R) were carried out in 500µl total volume according to the following conditions: 50µl of radioligand (fixed concentration), 100µl of membrane suspension and 350µl of test compound in increasing concentrations. Test-compounds were usually analyzed in five different concentrations (each in triplicate), spanning up to five orders of magnitude (p.e.10nM to 100µM). Chosen concentrations were adjusted appropriately for the IC50 of tested compounds. For an example of a typical experimental set- up see Table2.

Position	Compound	Conc.	Volume	[^{3}H]- DPCPX	Membrane	Temp.	Time
1-3	Buffer		350 µL	50 µL	100 µL	27°C	60min
4-6	DPCPX	1 µM	350 µL	50 µL	100 µL	27°C	60min
7-9	FE@SUPPY	0,01µM	350 µL	50 µL	100 µL	27°C	60min
10-12		0,1µM	350 µL	50 µL	100 µL	27°C	60min
13-15		1µM	350 µL	50 µL	100 µL	27°C	60min
16-18		10µM	350 µL	50 µL	100 µL	27°C	60min
19-21		100µM	350 µL	50 µL	100 µL	27°C	60min
22-24	MRS1523	0,01µM	350 µL	50 µL	100 µL	27°C	60min
25-27		0,1µM	350 µL	50 µL	100 µL	27°C	60min
28-30		1µM	350 µL	50 µL	100 µL	27°C	60min
31-33		10µM	350 µL	50 µL	100 µL	27°C	60min
34-36		100µM	350 µL	50 µL	100 µL	27°C	60min

Table 2: Experimental set- up: rack positions 1-3: control (determination of total binding), 4-6: determination of non- specific binding, 7-21 and 22-36 competitor in increasing concentrations

Vials containing radioligand, membrane suspension and competitor (see Figure 19a), were homogenized and then incubated at 27°C for 60 minutes (hA1R assay) or 90 minutes (hA2AR assay and hA3R assay) to achieve equilibration (Figure 19b). Immediately after incubation, samples were vacuum- filtrated using a cell harvester to separate the bound radioligand from the free (unbound) fraction. Glass fiber filters retained the radioligand-receptor-complex, whereas the unbound fraction (free radioligand) was filtered into the waste flask

(Figure 19c). Assay solutions were filtered through GF/B filters, which were presoaked in 0,5% PEI (hA1R assay and hA2AR assay) or 0,5% BSA (hA3R assay) for 10 minutes to reduce nonspecific binding.

Filter disks were punched out of the mat using and transferred to appropriate scintillation vials (Figure 19d). Radioactivity was determined for quantification of the receptor- bound fraction of the radioligand (Figure 19e). See Figure 19 for an overview of the working procedure.

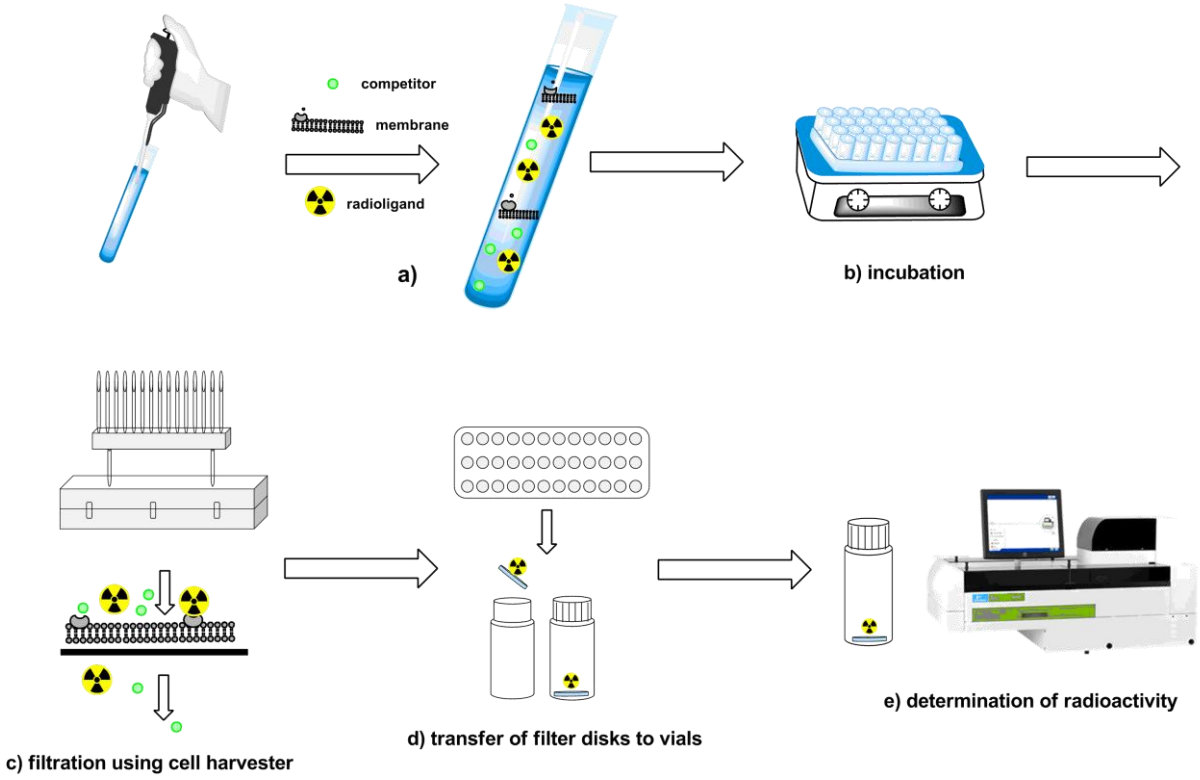

Figure 19: Scheme of radioligand binding assay

3.3.7 Counting of Radioactivity

In case of the **tritiated ligands [^{3}H]DPCPX** (hA1R assay) and **[^{3}H]CGS21680** (hA2AR assay) liquid scintillation counting was carried out, requiring the addition of 4ml scintillation fluid to each vial. Counting was conducted with a beta counter (HIDEX 300SL) under consideration of

the efficiency of the detected radioactivity. The efficiency is the fraction of the radioactive disintegrations, that is detected by the counter and was given by the manufacturer with up to 72%. The actual concentration of radioligand had to be calculated. Therefore, the specific activity (in Ci/mmol) was converted to cpm/fmol, as radioactivity is measured in counts per minute (see Figure 20).

$$\mathrm{Y}\frac{\mathrm{cpm}}{\mathrm{fmol}} = \mathrm{Z}\frac{\mathrm{Ci}}{\mathrm{mmol}} \times 2{,}22 \times \mathrm{E}$$

$$35{,}02\,\frac{\mathrm{Ci}}{\mathrm{mmol}} \times 2{,}22 \times 0{,}72 = 55{,}975\,\frac{\mathrm{cpm}}{\mathrm{fmol}}$$

Figure 20: Conversion of specific activity stated in Ci/mmol to cpm/fmol. 1 Curie equals 2.22×10^{12} disintegrations per minute and E is the efficiency of the counter. [31] For demonstration, one example was calculated based on [^{3}H]CGS21680 (specific activity of 35.02Ci/mmol), which was used in a concentration of 50nM in 500µl end volume.

Then the actual concentration of radioligand (pM) was calculated via total count and used volume (see Figure 21).

$$\mathrm{Conc\ RL\ (pM)} = \frac{\mathrm{C}\ /\ \mathrm{Y}}{\mathrm{V}}$$

$$\frac{1.160.000/55{,}975}{0{,}5} = 41447\ \mathrm{pM}$$

Figure 21: C is a standard sample of 50nM [^{3}H]CGS21680 in 0.5ml (V), denoted as total count (cpm) and was determined under the same conditions to those used in the experiments. Y is the specific activity in cpm/fmol, calculated previously. [31]

In this example, the actual concentration of [^{3}H]CGS21680 present in the assay probes amounts to 41.4nM and had to be used for the calculation of K_i values see Figure 22.

$$K_i = \frac{IC50}{1 + \frac{[RL]}{K_d}} = \frac{28{,}75}{1 + \frac{41{,}4}{23}} = 10{,}26\text{nM}$$

Figure 22: Calculation of K_i value, using the actual concentration of radioligand ([^{3}H]CGS21680) calculated previously. The IC_{50} of competitor, the K_d value, and the concentration of radioligand are stated in nM. [27] IC_{50} was obtained by analyzing radioligand binding data using the GraphPad Prism® Software (see 3.3.7).

Radioactivity of the **iodinated ligand [^{125}I]AB-MECA** was determined via gamma counting. Generally, the efficiency of the used gamma counter with ^{125}I is greater than 90% and can therefore be ignored. However, with ^{125}I one has to consider radioactive decay (see calculation in section 3.3.2).

For an overview of the main parameters of radioligand binding assays using membrane target systems™ see Table 3.

Membrane Target System PerkinElmer®	hA1R	hA2AR	hA3R
Protein concentration	18.5ng/µl	16.7ng/µl	1.7ng/µl
Radioligand	[^{3}H]DPCPX	[^{3}H]CGS21680	[^{125}I]AB-MECA
Concentration of radioligand	1.7nM	50nM	0.4nM
Activity concentration	37MBq/ml	37MBq/ml	5.89MBq/ml
Determination of nonspecific binding	1µM DPCPX	1µM SCH442416	10µM I-AB-MECA
Incubation	60min (27°C)	90min (27°C)	60min (27°C)
Filtration	GF/B Whatman®	GF/B Whatman®	GF/B Whatman®
Determination of radioactivity	Liquid Scintillation Counting	Liquid Scintillation Counting	Gamma-Counter

Table 3: Main parameters of radioligand binding assays.

3.3.8 Analysis of Data

The analysis of the data was conducted using the GraphPad Prism® Software. Determination of the radioactivity led to the quantification of the bound fraction of radioligand. For generation of competitive binding curves logarithmic concentrations of test compound were plotted on x axis and binding values of radioligand (cpm) on y axis. Probes were analyzed in triplicates (Y1-Y3) and mean values were calculated (Figure 23).

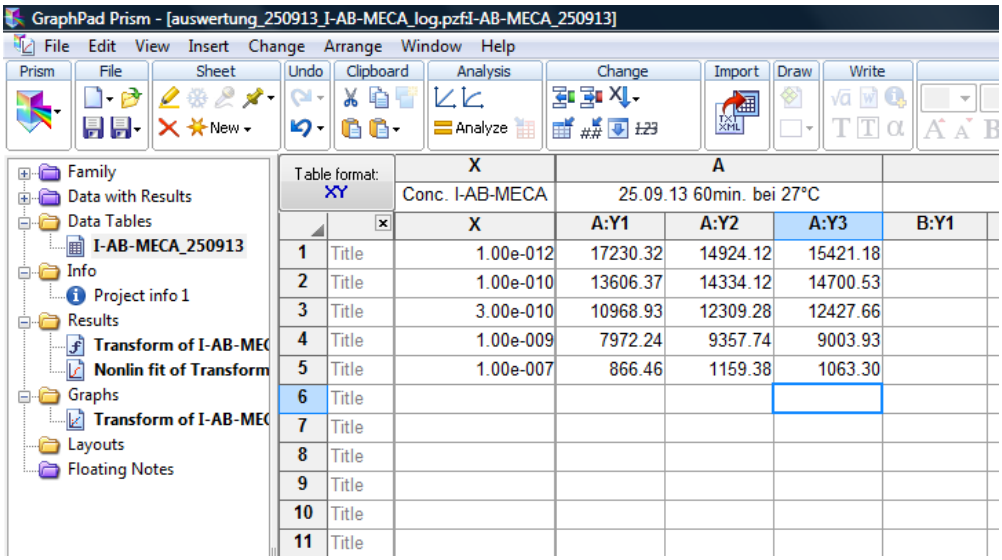

Figure 23: Analyzing radioligand binding data using the GraphPad® Prism Software.

Subsequently, under the item "*Analyze*" the function "*Transform of*" was elected. X values (concentrations of test compound) were transformed as "*X=logX*" (see Figure 24).

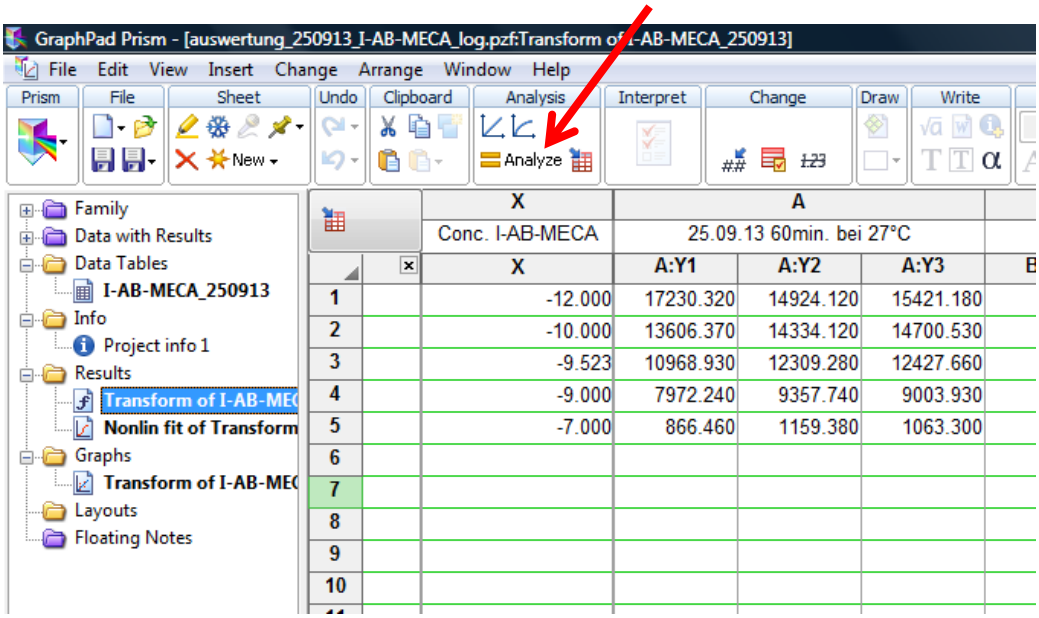

Figure 24: Transformation of x values.

Competitive binding curves (Figure 25) were obtained by analyzing binding data using the function: "*log(inhibitor) vs response –variable slope"*.

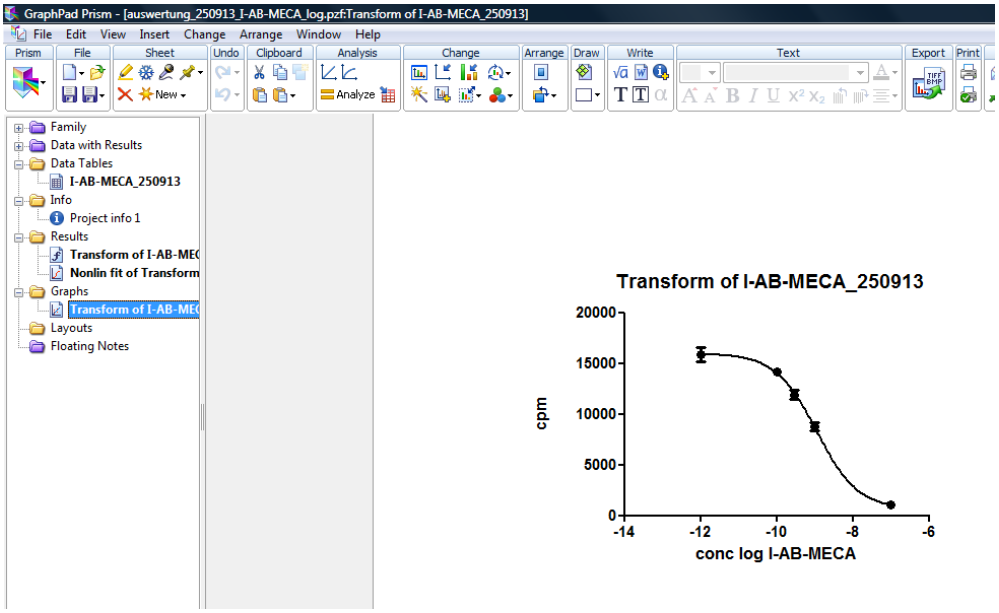

Figure 25: Competitive binding curve obtained by using GraphPad Prism® Software.

IC50 values and hillslope were obtained (see Figure 26). Hillslope refers to the steepness of the binding curve and should be around -1.

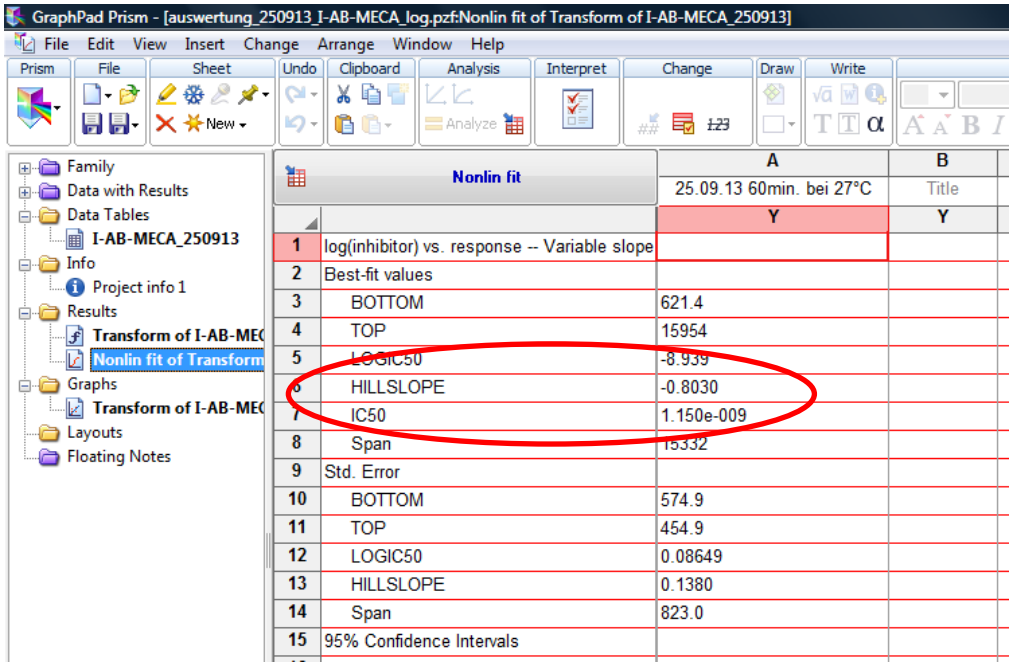

Figure 26: IC50 was obtained by analyzing radioligand binding via the GraphPad Prism® Software

The received IC50 was inserted in the calculation of the respective K_i value using the Cheng&Prusoff equation (see Figure 13 in 1.2.1).

4. RESULTS

4.1 ANALYSIS OF DATA

Table 4 shows an overview of the obtained results of the assays hA1R, hA2AR and hA3R, each conducted with the compounds: FE@SUPPY, FE@SUPPY:2, FE@SUPPY:11, FEMe@SUPPY:2, FE^2@SUPPY, Me^2@SUPPY, DFE@SUPPY, DFE@SUPPY:2, FE@CAPPY, Me^2@CAPPY, BD1, BD3, MRS1191 and MRS1523.

compound	hA1R Ki[nM]	hA2AR Ki[nM]	hA3R Ki[nM]	hA1R/hA3R	hA2AR/hA3R
FE@SUPPY	4029±1056 (n=5)	1717±365 (n=3)	6.02±0.4 (n=3)*	669	285
FE@SUPPY:2	2701±1047 (n=3)	1552±7 (n=2)	8.3±0.9 (n=2)** 32.5±5 (n=2)*	325 83	187 48
FE@SUPPY:11	≥ 57240 (n=2)	5862±815 (n=3)	2800±1430 (n=3)*	20	2
FEMe@SUPPY:2	3086±770 (n=2)	3232±2654 (n=2)	87.9±12 (n=2)*	35	37
FE^2@SUPPY	5035±2060 (n=3)	1741±229 (n=4)	15.5±6 (n=3)**	324	112
Me^2@SUPPY	2620±734 (n=3)	1292±412 (n=3)	272.2±23 (n=2)* 6.1±5 (n=2) **	10 430	5 212
DFE@SUPPY	5457±358 (n=2)	37134±16344 (n=3)	2578±1195 (n=3)*	2	14
DFE@SUPPY:2	3306±364 (n=2)	1481±579 (n=3)	≥ 2350 (n=2)*	1.4	0.6
FE@CAPPY	11129±8826 (n=3)	28858 (n=1)	29.1±3 (n=2)**	382	992
Me^2@CAPPY	3192±2463 (n=2)	1372±1052 (n=3)	45.7±18 (n=2)**	70	30
BD1	3874±278 (n=3)	18248±14970 (n=3)	≥2671 (n=2)**	1.5	7
BD3	12765±3975 (n=3)	50661±19447 (n=3)	≥6401 (n=2)**	2	8
MRS1523	4603±1735 (n=3)	528±214 (n=4)	33.9±15 (n=3)*	136	16
MRS1191	131737±14395 (n=2)	29644±11842 (n=2)	40.9 (n=1)**	3221	725

Table 4: K_i values were obtained by radioligand binding assays using Brandel® Cell Harvester as described. Different solubility of compounds led to different concentrations of DMSO in stock solutions and therefore at maximum 10% DMSO in total volume of some assay probes; *) DMSO ≤1% **) DMSO ≤ 10%

4.1.1 Proof of Method

For every membrane each pharmacological model substance (ligand) was evaluated according to the manufacture´s sheet for respective membrane target systems™ (see appendix). Correlation of obtained experimental K_i values with respective K_i values from Technical Data Sheets is shown in Table 5.

Ligand	Membrane target system™	Ki experimental [nM]	Ki literature [nM]
DPCPX	hA1R	1.7 ±0.6	1.7
CGS21680	hA2AR	14.02±3	23
I-AB-MECA	hA3R	1.06±0.6	0.78

Table 5: Proof of method: reference values were taken from the Technical Data Sheets (Membrane Target Systems™, PerkinElmer®) of the respective labeled ligands. K_i values [nM] are means of at least three experiments ± standard deviation

4.1.2 Binding Data of the Lead Compounds FE@SUPPY and FE@SUPPY:2

FE@SUPPY displays a K_i value of 6.02nM±0.4 for the hA3R and low affinity towards the other subtypes (K_i=4µM±1 (hA1R) and K_i=1.7µM±0.3 (hA2AR)) (see Table 6, Figure 27-28). FE@SUPPY shows high hA3R selectivity towards the hA1R and the hA2AR (with ratios of 669 and 286).

	Ki [nM]			ratios	
	hA1R	hA2AR	hA3R	hA1R/hA3R	hA2AR/hA3R
	2769,03286	2137,78604	6,4522	669,00198	285,05677
	3349,17299	1492,08859	5,6383		
	4801,34034	1520,16062	5,9762		
	5364,95158		6,4522		
	3859,93243				
MW	4028,88604	1716,67842	6,02223333		
STABW	1055,88138	364,959906	0,40889804		

Table 6: K_i values of FE@SUPPY are means of 3-5 experiments. K_i values (hA3R) were obtained using wash buffer for diluting, leading to a content of DMSO lower than 1% in total volume. 100µM dilutions of FE@SUPPY, used within A1R and A2AR assay, were obtained using DMSO for solubilizing (10% in final volume).

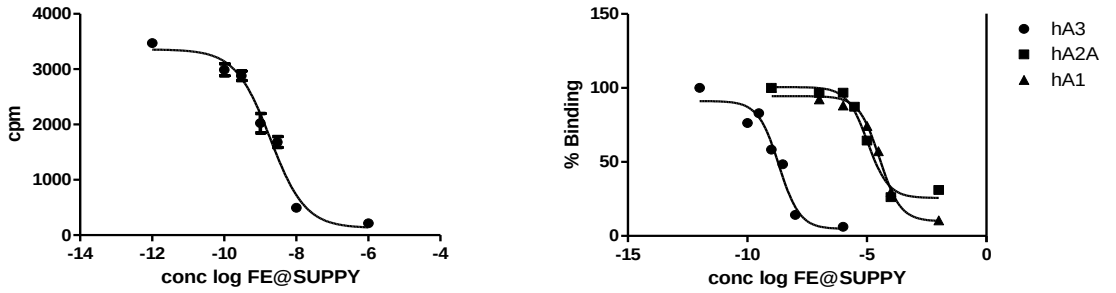

Figure 27: Representative competitive curve of FE@SUPPY using hA3R membrane and [^{125}I]AB-MECA is shown in the left graph. The right graph shows IC_{50} fitted binding curves of FE@SUPPY at hA3R, hA2AR, hA1R and demonstrates high affinity of FE@SUPPY towards hA3R.

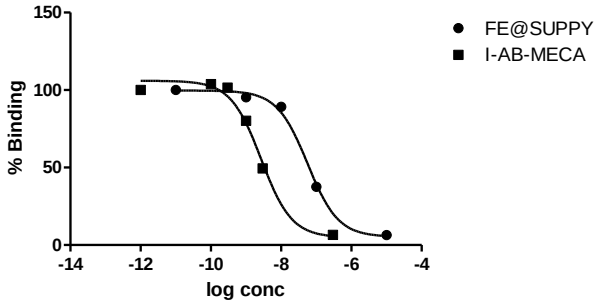

Figure 28: Competitive binding curves of [^{125}]I-AB-MECA at hA3R using FE@SUPPY and I-AB-MECA as competitor.

For FE@SUPPY:2 K_i values (hA3R) in one fold nM range (8.3nM±0.9 (n=2)) were obtained, when deionized water was used for diluting and DMSO was added as a solubilizer at a content of 10% in total volume (see Figure 29).

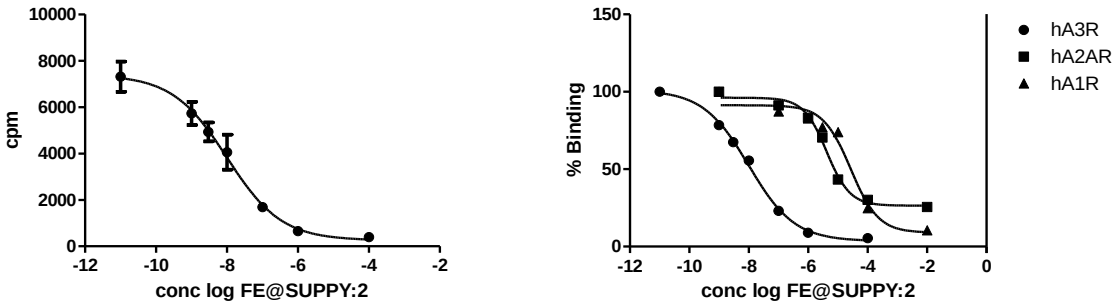

Figure 29: In the left graph a representative binding curve of FE@SUPPY:2 is shown; obtained by the parameters mentioned above. The right graph shows the comparison of competitive binding curves of FE@SUPPY:2 at hA3R, hA2AR and hA1R, demonstrating good affinity towards hA3R.

Using Tris buffer and a content of DMSO <1% for dilution, led to higher K_i values (32.5nM±5 (n=2)) for FE@SUPPY:2 towards hA3R.

FE@SUPPY:2 shows low affinity towards the other subtypes; as K_i values in micromolar range were obtained (K_i=3.3µM±0.3 (hA1R) and K_i=1.6µM±0 (hA2AR), respectively).

4.1.3 Binding Data of the Metabolites DFE@SUPPY and DFE@SUPPY:2

The respective metabolites of FE@SUPPY and FE@SUPPY:2 do not show any affinity at the hA3R (K_i≥1.3µM for DFE@SUPPY (ranging from 1.3 to 3.7µM) and K_i≥2.4µM for DFE@SUPPY:2 (ranging from 2.4 to 6.9µM)) as well as no selectivity towards the other subtypes (see Table 4, Figure 30-31).

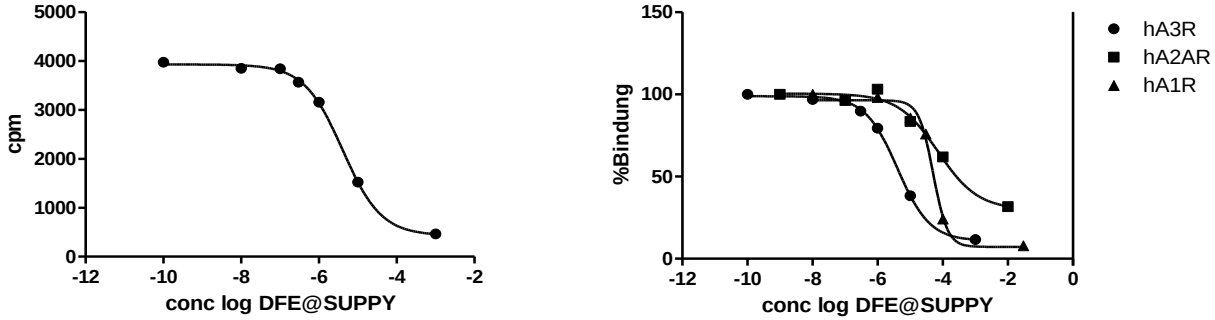

Figure 30: Left graph: Representative binding curve of DFE@SUPPY using hA3R expressing membrane. Displacement of [^{125}I]AB-MECA occurred only at 10µM of DFE@SUPPY. Right graph: Competitive binding curves of DFE@SUPPY using hA3R, hA2AR and hA1R membranes.

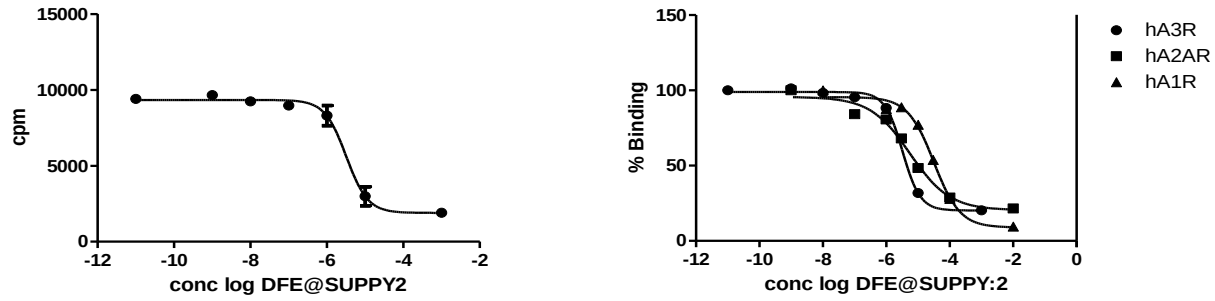

Table 31: Left graph: Representative binding curve of DFE@SUPPY:2 using hA3R expressing membrane. Displacement of [^{125}I]AB-MECA occurred only at 10µM of DFE@SUPPY:2. Right graph: Competitive binding curves of DFE@SUPPY:2 using hA3R, hA2AR and hA1R membranes.

4.1.4 Binding Data of the New FE@SUPPY- Derivatives (FEMe@SUPPY:2, FE@SUPPY:11, FE^2@SUPPY, Me^2@SUPPY)

FEMe@SUPPY:2 shows intermediate affinity for hA3R, as K_i values in two fold nanomolar range were obtained under following conditions: 96.5nM (using Tris buffer for diluting test compound at a content of ≤0.1% DMSO in final volume), 79.4nM (using deionized water for diluting test compound at a content of 3.8% DMSO) and 21.6nM (using deionized water for diluting test compound at a content of up to 10% DMSO).

FE@SUPPY:11 does not show affinity for hA3R (K_i=2800nM±1430), neither when test compound was diluted in assay buffer (K_i=1392nM), nor in Tris buffer (K_i=4251nM and 2758nM) (in each case content of DMSO was ≤1%).

For determination of the K_i value (hA3R) of FE^2@SUPPY, test compound was dissolved in deionized water at a content of 2% DMSO (1µM dilution) and ≤0,2% DMSO (dilutions ≤ 100nM) respectively. Thus, K_i values of 21.9nM and 14.3nM were obtained. Even if assay buffer was used for conduction of dilution, a K_i value in the same range (10.2nM) was obtained (see Figure 32).

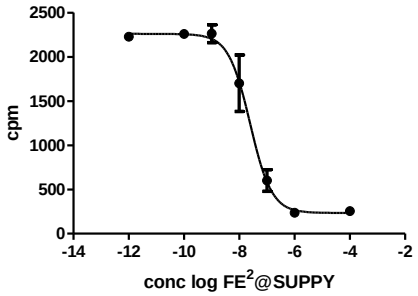

Figure 32: Representative competitive binding curve of FE^2@SUPPY at the hA3R obtained with parameters described above, leading to a K_i value of 15.5nM±6 (n=3).

In contrast, when wash buffer (50mM Tris- HCl, pH 7.4) was used for dilution of FE^2@SUPPY no displacement of radioligand ([^{125}I]AB-MECA) occurred (n=2).

For Me^2@SUPPY K_i values in three fold nanomolar range (255.9nM and 288.4nM) were obtained at hA3R, when standard solutions were made using wash buffer (50mM Tris- HCl, pH 7.4) at a content of DMSO ≤1% in final volume. K_i values in one fold nanomolar range (9.42nM and 2.86nM) were obtained, when DMSO was raised to 3,4% DMSO (1µM dilution) and solutions were made using deionized water.

None of the new FE@SUPPY- derivatives showed affinity towards the adenosine receptor subtypes A1R and A2AR, as K_i values in micromolar range were obtained (see Table 4).

4.1.5 Binding Data of Structurally Related Ligands (FE@CAPPY, Me^2@CAPPY) and Structurally Different Ligands (BD1, BD3)

FE@CAPPY shows intermediate affinity at the hA3R, as K_i values in two fold nanomolar range were obtained (K_i= 27.2nM and 30.9nM) (test compound was diluted in deionized water at a content of ≤10% DMSO). FE@CAPPY does not show affinity towards hA1AR (K_i=11.1µM±9) as well as towards hA2AR (K_i=28.9µM). In case of hA2AR assay due to limitations of the method only one out of four experiments was analyzable (see discussion 5.1).

Me^2@CAPPY shows K_i values in two fold nanomolar range for hA3R; 58.6nM (using Tris buffer at a content of DMSO lower than 1%) and 32.8nM (deionized water for diluting at a content of 1-10% DMSO). Otherwise, a K_i value of 308.8nM was obtained, when omitting the addition of DMSO.

BD compounds (BD1, BD3) were dissolved in Tris buffer (50mM, pH 7.4) or water (sterile, deionized) at a content of DMSO ≤1% in final volume. Under these conditions displacement of [^{125}I]AB-MECA was observed only at 10µM and K_i values for hA3R are therefore estimated as ≥2,7µM (BD1)and ≥6,4µM (BD3) (see Figure 33).

Following K_i values were obtained for the other subtypes; BD1: 3.9µM±0.3 (n=3) at hA1R and 18.2µM±15 (n=3) at A2AR and BD3: 12.8µM±4 (n=3) at hA1R and 50.7±19 (n=3) at hA2AR. The BD compounds do not show affinity for any of the human adenosine receptor subtypes and therefore no selectivity towards hA3R (see Figure 34).

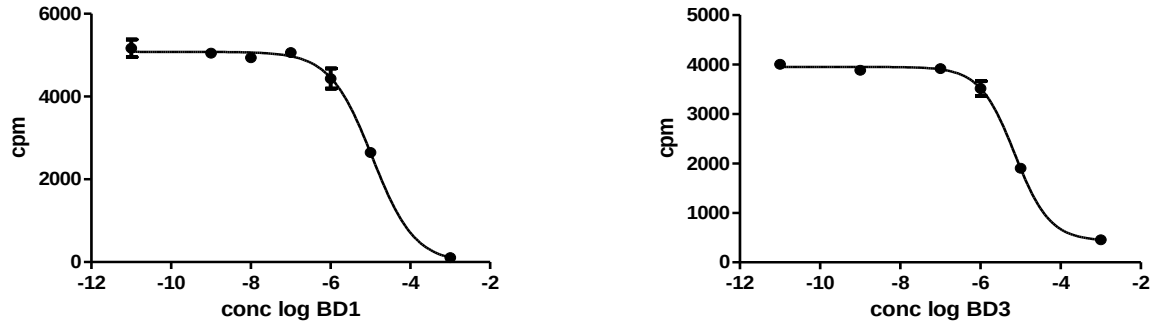

Figure 33: Competitive binding curve of BD1 (shown in the left graph) and BD3 (shown in the right graph) at hA3R. Displacement of the radioligand occurred only when 10^{-5}M (10µM) of competitor (BD1 or BD3) was applied. Lower concentrations did not led to a displacement of [^{125}I]AB-MECA.

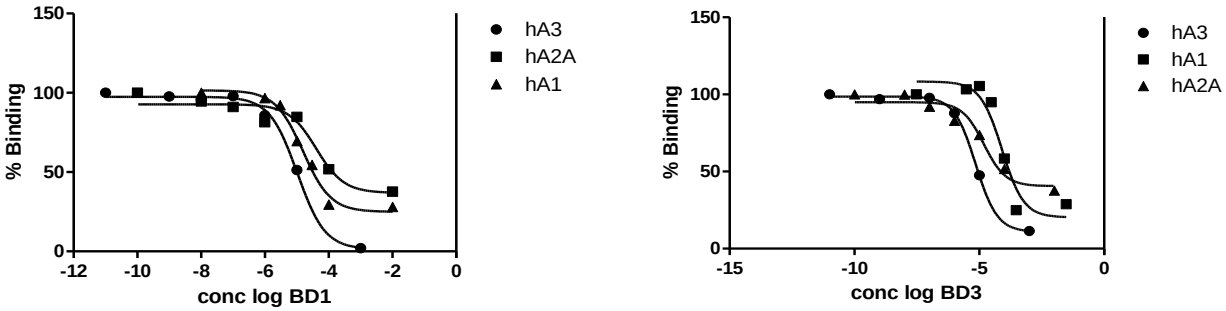

Figure 34: In the left graph competitive binding curves of BD1 at hA3R, hA2AR and hA1R are shown. In the right graph competitive binding curves of BD3 at hA3R, hA2AR and hA1R are shown.

4.1.6 Binding Data of Reference Compounds (MRS1523, MRS1191)

For MRS1523 a K_i value of 33.9nM±15 was obtained for hA3R. Low affinity was observed for the hA1R with a K_i value of 4.6µM±1.7. Regarding the hA2AR, MRS1523 showed intermediate affinity (528nM±214), leading to no appreciable selectivity towards hA3R (ratio hA2AR/hA3R= 16).

Following results were obtained, concerning MRS1191 and the hA3R: When test compound was diluted in wash buffer (50mM Tris-HCl, pH 7.4), no displacement of radioligand was observed (n=5). Degradation of MRS1191 and defect membrane preparation could be excluded as the cause, since new batches were ordered. When MRS1191 was diluted in deionized water (DMSO ≤10%), a K_i value of 159.2nM±54 (n=2) was obtained. Using assay buffer (see 3.3.4 for composition of assay buffer) for dilution, led to a K_i value of 40.9nM (DMSO ≤10%). MRS1191 does not show affinity for the other subtypes with K_i values of 131.7µM±14 (hA1R) and 29.6µM±12 (hA2AR).

5. DISCUSSION

5.1 PREPARATION OF STOCK SOLUTIONS AND DILUTION SERIES OF COMPOUNDS

Within the 100µM dilutions of the various competitors, the addition of DMSO was necessary up to a content of 10% in final volume to ensure a complete solution of the compounds. Due to the lipophilicity of some test compounds and the associated limited solubility in water, concentrated solutions (higher than 100µM), containing a maximum of 10-15% of DMSO, were not feasible. Within the A1R assay and A2AR assay high concentrated dilutions (≥100µM) of competitor (BD1, BD3, FE@CAPPY, MRS1191 and FE@SUPPY:11) were required to achieve displacement of radioligand, since the compounds displayed low affinity for this receptors. Therefore, a complete displacement of radioligand was not possible and the limit of detection of this method was reached.

The addition of DMSO exhibited direct effects on the obtained K_i value. It was observed that, higher contents of DMSO (up to 10%) provoked lower K_i values, presumably due to the improvement of solubility of the test compound. This phenomenon was most blatant with Me^2@SUPPY, as K_i values in three fold nanomolar range versus one fold nanomolar range were obtained (see 4.1.4). Similar results were observed for Me^2@CAPPY (K_i values in three fold nanomolar range versus two fold nanomolar range, see 4.1.5), FE@SUPPY:2 (K_i values in two fold versus one fold nanomolar range, see 4.7.2) and FEMe@SUPPY:2 (steady decline of K_i values by rising DMSO content, see 4.1.4).

Obviously, the addition of DMSO to the assay probes contributes significantly to the solubility of the tested compounds, since Me^2@SUPPY, Me^2@CAPPY and FEMe@SUPPY:2 are relative high lipophilic compounds, as they comprise two ester moieties (different to those, that have one free thio- or carboxylic-acid respectively).

Since the addition of DMSO to improve solubility is unphysiological and hence smaller K_i values are simulated, concentrations of DMSO higher than 2% in assay probes should be avoided. Otherweise, one gets “fake” affinity values, which are not displayed by the

compound itself but from the DMSO and will therefore not bind with this low K_i *in vivo*. Therefore, we decided for those values with low proportion of DMSO and excluded data obtained with higher DMSO concentrations.

Moreover, the influence of the solvent (dilution medium) was investigated in more detail. In some cases experiments did not work at all using 50mM Tris- HCl (pH 7.4) buffer for dilution, as it was observed for example for FE^2@SUPPY. In contrast, FE@SUPPY could be reproduced successfully at the first attempt, using 50mM Tris- HCl (pH 7.4) buffer for dilution (see Table 5 in 5.3).

Within one experimental set-up, MRS1191 was dissolved either in deionized water or in assay buffer (see 3.3.4 for composition of assay buffer) (each with an amount of DMSO ≤10%), in order to analyze the effect of the used solvent by limiting all external influence factors (see Graph 35).

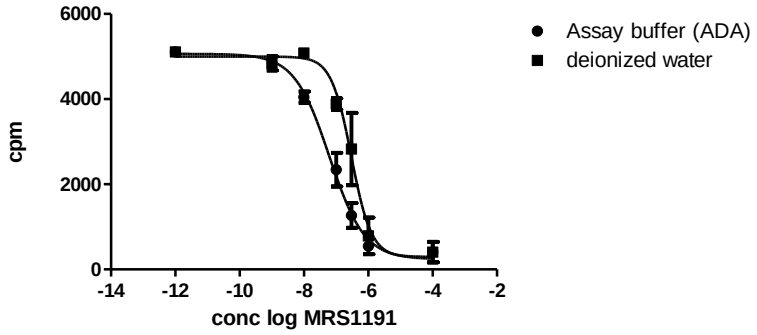

Table 35: IC_{50} fitted binding curves of MRS1191 using [^{125}I]AB-MECA and hA3R expressing membrane. Diluting MRS1191 in assay buffer led to a K_i value of 40.9nM, whereas when using deionized water for dilution, a K_i value of 197.5nM was obtained for MRS1191.

Due to solubility differences of the tested compounds, it was not possible to elicit a solvent, which was optimal and suitable for all test compounds.

5.2 Composition of Buffer

The addition of adenosine deaminase to the assay buffer was essential within the A2AR assay, but not within A1R or A3R assay. Within the A2AR assay, endogenous adenosine was present in the membrane preparation. Unfortunately, no information about the actual adenosine concentration could be obtained from the manufacturer (PerkinElmer®). Interestingly, adenosine deaminase was not obligatory and necessary to add for the other assays (hA1R, hA3R).

Due to structural similarities to adenosine, it has to be considered that [^{125}I]AB-MECA and [^{3}H]CGS21680 may be substrate of ADA, since both ligands comprise the purine base adenine (see Figure 36). However, degradation of radioligands by ADA could not be confirmed, as no significant decrease in radioactivity was observed when ADA was added to the buffer versus no ADA.

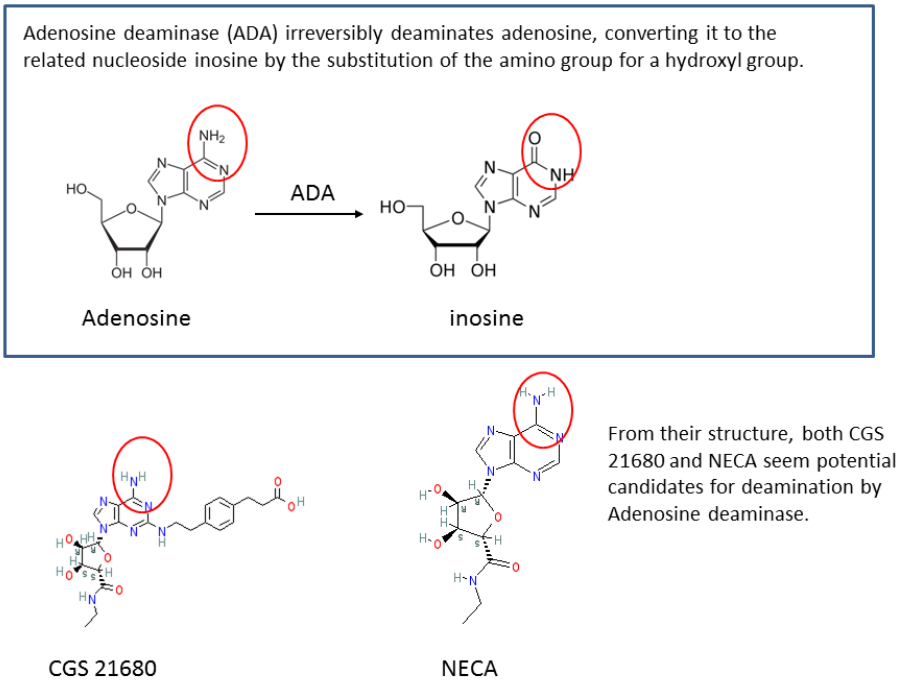

Figure 36: Degradation of adenosine to inosine by adenosine deaminase, as it happens physiologically, is shown in the top of the figure. Due to structurally similarities, CGS21680, NECA as well as I-AB-MECA (all display the purine base adenine) may be potential substrates of ADA.

5.3 Binding Data

Unlike the cold ligands (I-AB-MECA, DPCPX, CGS21680), K_i values of reference compounds (MRS1523 and MRS1191 for hA3R) could not be easily reproduced. Experiments with MRS1523 had an extraordinary high default rate, but finally the K_i value, published in literature could be reproduced in an acceptable manner. MRS1191 was even more problematic to reproduce according to literature´s K_i. When MRS1191 was diluted in deionized water, a K_i value of 159.2nM±54 (n=2) was obtained, which is far away from literature. Using assay buffer for dilution, led to a K_i value of 40.9nM, which comes close to literature (see Table 5).

Ligand	Receptor	Ki [nM]	
		taken from Refs	this work
I-AB-MECA	hA3	0.78 [a)]	1.06 ±0.6 (n=6)
FE@SUPPY	hA3	4.2 [b)]	6.02±0.4 (n=3)
MRS1523	hA3	18.9 [c)]	39.9±15 (n=3)
MRS1191	hA3	31.4 [d)]	40.9 (n=1)
CGS21680	hA2A	23 [a)]	14.02±3 (n=3)
DPCPX	hA1	1.7 [a)]	1.73±0.6 (n=4)

Table 5: For proof of method, K_i values derived from literature were reproduced in a reasonable range. a) K_i values for respective radiolabeled ligands were taken from technical data sheets PerkinElmer® (see appendix). b) Li et al., *J Med Chem*. 1999, 42 c) Li et al., *J Med Chem*. 1998, 41 d) Jiang et al., *J Med Chem*. 1996, 39

Interestingly, K_i values of FE@SUPPY, MRS1191 and MRS1523 were obtained using DMSO at a content ≤2%, as it is stated by the authors: *"All nonradioactive compounds were initially dissolved in DMSO and diluted with buffer to the final concentration, where the amount of DMSO never exceeded 2%."* [9],[10],[11]

None of the tested compounds display affinity for the hA1R and hA2AR. Some show affinity for the hA3R.

The high affinity of FE@SUPPY, our lead compound was verified in this thesis with a K_i value of 6.02nM±0.4 in comparison to the literature with a K_i of 4.2nM [10]. Among all tested compounds, FE@SUPPY still displays the lowest K_i value in regard of the hA3R and therefore the highest affinity for the human A3R. Furthermore, a remarkably selectivity (669 fold towards human A1R and 286 fold towards human A2AR) was discovered. Therefore, FE@SUPPY shows the best binding profile regarding its affinity and selectivity towards the hA3R. FE@SUPPY:2 displayed less favorable K_i values in a one fold to two fold nanomolar range (K_i= 8.3nM±0.9 and 32.5nM±5, respectively). Moreover, selectivity is not as high as observed for FE@SUPPY; with ratios of hA1R/hA3R <396 and hA2AR/hA3R <187.

Among the new FE@SUPPY-derivatives, FE^2@SUPPY turned out as a potent A3R antagonist (K_i=15.5nM±6), however its binding profile is not as good as FE@SUPPY (see Table 4). Me^2@SUPPY does not show affinity for the hA3R, since K_i values in three-fold nanomolar range were obtained. Me^2@SUPPY, comprises two methylesters and therefore lacks the flourethyl residue, which was expected to contribute mainly to the affinity towards A3R. FEMe@SUPPY:2, which comprises one flourethylester and one methylester, showed intermediate affinity for the hA3R.

DFE@SUPPY and DFE@SUPPY:2 are the potential metabolites of the respective PET-tracers [^{18}F]FE@SUPPY and [^{18}F]FE@SUPPY:2. They do not show affinity for the hA3R, which is an advantage for potential future clinical application.

FE@SUPPY:11, which is structurally similar to DFE@SUPPY and DFE@SUPPY:2, since they all comprise a free acid, does not show affinity for the hA3R either.

FE@CAPPY and Me^2@CAPPY, which are structurally related to the FE@SUPPY- derivatives (two carboxylester moieties) show both intermediate affinity (K_i values of 29.1nM±3 and 45.7nM±18, respectively) towards the hA3R.

BD1 and BD3, compounds which are chemically distinct to the FE@SUPPY-series, seem not to target adenosine receptors at all and therefore do not contribute an alternative and will not be further pursued.

The importance of this work is evident by the fact that to date no data regarding selectivity towards the human A3R versus the human A2AR and human A1R were available. For

FE@SUPPY only the ratio hA3R versus rat A1R was published by Li et al (rA1/hA3R= 2700). [10] It should be emphasized that, selectivity for the FE@SUPPY-derivatives was evaluated for the first time.

6 CONCLUSION & OUTLOOK

The A1R assay functioned at first attempt and values could be reliably reproduced over a long time period. For the A2AR assay, the presence of adenosine deaminase was crucial during incubation. Interestingly, the hA3R assay turned out to be a very sensitive and instable system. Assay parameters were thoroughly evaluated, wherein the chosen solvent for dilution of test compound as well as the added amount of solubilizer (DMSO) turned out to be crucial. The limitations of the method consisted in the poor solubility of some compounds. One of the most striking findings of this binding study was the tremendous influence of DMSO in compound solutions on the respective K_i values. As higher contents of DMSO (up to 10%) in assay probes led to lower K_i values than respective K_i values obtained when using ≤1% DMSO. Moreover, one has to consider that, the addition of DMSO as a solubilizer is an unphysiological process and should therefore be avoided if possible.

BD1, BD3, FE@SUPPY:11, DFE@SUPPY and DFE@SUPPY:2 showed human A3R K_i values in a µM range and therefore do not represent potential A3R antagonists. FE@CAPPY, Me^2@CAPPY, Me^2@SUPPY and FEMe@SUPPY:2 showed intermediate to low affinity for the hA3R and are insufficient for a potential PET-tracer regarding their affinity. FE^2@SUPPY turned out as a new potential candidate, since this compound shows relative high affinity for the hA3R and good selectivity towards the other subtypes. However, FE@SUPPY shows the best binding profile among all tested compounds.

A positive finding regarding pharmacokinetics of our potential PET-tracers, is, that the respective metabolites DFE@SUPPY and DFE@SUPPY:2 do not show any affinity for the hA3R.

This thesis confirmed once more the potential of FE@SUPPY to serve as a future PET-Tracer, as FE@SUPPY displays an outstanding binding profile (best affinity and selectivity) among a pool of new derivatives. Therefore, a new project, dealing with the evaluation of [^{18}F]FE@SUPPY for oncology, which was recently funded by the Austrian Science Fund (FWF P26502-B24, awarded to M. Mitterhauser) will be the next step.

7 REFERENCES

[1] Poulsen SA. Quinn RJ. Adenosine receptors: New opportunities for Future Drugs. 1998 *Bioorg Med Chem*; 6:619-41

[2] Introduction to Adenosine Receptors as Therapeutic Targets. Jacobson KA. In: Wilson CN, Mustafa SJ, editors. Adenosine Receptors in Health and Disease. Springer 2009, 4-19

[3] Fredholm BB, Ijzerman AP, Jacobson KA. International Union of Pharmacology. XXV. Nomenclature and Classification of Adenosine Receptors. 2001 *Pharmacol Rev;* 53:527-52

[4] Moro S, Spalluto G, Jacobson KA. Techniques: Recent developments in computer-aided engineering of GPCR ligands using the human adenosine A_3 receptor as an example. 2005 *Trends Pharmacol Sci*; 26:44-51

[5] Gao Z, Jacobson KA. Adenosine receptors as therapeutic targets. 2006 *Nature rev drug discovery*; 5:247-64

[6] Benarroch EE. Adenosine and its receptors: multiple modulatory functions and potential therapeutic targets for neurologic disease. 2008 *Neurology*; 70: 231-6

[7] Madi L, Ochaion A, Rath- Wolfson L. The A_3 adenosine receptor is highly expressed in tumor versus normal cells: potential target for tumor growth inhibition. 2004 *Clin Cancer Res*; 10:4472-9

[8] Gessi S, Cattabriga E, Avitabile A. Elevated expression of A3 adenosine repetors in human colorectal cancer is reflected in peripheral blood cells. 2004 *Clin Cancer Res*; 10:5895-901

[9] Gessi S, Merighi S, Sacchetto V, Simioni C, Borea PA. Adenosine receptors and cancer. 2011 *Biochim Biophys Acta*; 1808: 1400-1412

[10] Fishman P, Bar-Yehuda S, Synowitz M, Powell JD, Klotz KN, Gessi S and Borea PA. Adenosine receptors and cancer. In: Adenosine Receptors in Health and Disease. Wilson CN, Mustafa SJ, Springer 2009

[11] Fishman P, Bar- Yehuda S, Varani K. Part VII Cancer. Agonists and Antagonists: Molecular Mechanisms and Therapeutic Applications. In: Borea PA. A3 Adenosine Receptors from Cell Biology to Pharmacology and Therapeutics. Springer 2010; 301-17

[12] Zhou QY, Li C, Olah ME. Molecular cloning and characterization of an adenosine receptor: the A3 adenosine receptor. 1992 *Proc Natl Acad Sci* USA; 89:7432-36

[13] Salvatore CA, Jacobson MA, Taylor HE. Molecular cloning and characterization of the human A3 adenosine receptor. 1993 *Proc Natl Acad Sci* USA; 90:10365-69

[14] Baraldi PG, Cacciari B, Romagnoli R. A_3 Adenosine Receptor Ligands: History and Perspectives. 2000 *Med Res Rev*; 20:103-28

[15] Jiang J, Van Rhee AM, Melman N. 6-Phenyl-1,4-dihydropyridine derivatives as potent and selective A3 adenosine receptor antagonists. 1996 *J Med Chem*; 39: 4667-75

[16] Li AH, Moro S, Forsyth N. Synthesis, CoMFA Analysis, and Receptor Docking of 3,5-Diacyl-2,4-Dialkylpyridine Derivatives as Selective A3 Adenosine Receptor Antagonists. 1999 *J Med Chem*; 42: 706-21

[17] Li AH, Moro S, Melman N. Structure-activity relationships and molecular modeling of 3,5-diacyl-2,4-dialkylpyridine derivatives as selective A3 adenosine receptor antagonists. 1998 *J Med Chem*; 41:3186-201

[18] Wadsak W, Mien LK, Shanab K, et al. Radiosynthesis of the adenosine A3 receptor ligand 5-(2-[18F]fluoroethyl)2,4-diethyl-3-(ethylsulfanylcarbonyl)-6-phenylpyridine-5-carboxylate ([18F]FE@SUPPY). 2008 *Radiochim Acta*; 96: 119-24

[19] Wadsak W, Mien LK, Shanab K, et al. Preparation and first evaluation of [18F]FE@SUPPY: a new PET-tracer for the adenosine A3 receptor. 2008 *Nucl Med Biol*; 35:61-6

[20] Mitterhauser M, Haeusler D, Mien LK. Automatisation and first evaluation of [18F]FE@SUPPY:2, an alternative PET-tracer for the adenosine A3 receptor: a comparison with [18F]FE@SUPPY. 2009 *The Open Nuclear Medicine Journal*; 1:15-23

[21] Haeusler D, Nics L, Mien LK. [18F]FE@SUPPY and [18F]FE@SUPPY:2 – metabolic considerations. 2010 *Nucl Med Biol*; 37:421-26

[22] Motulsky HJ. Mahan LC. The kinetics of competitive radioligand binding predicted by the law of mass action. 1984 *Mol Pharmacol*; 25:1-9

[23] The law of mass action. In: The GraphPad Guide to Analyzing Radioligand Binding Data. Dr. Harvey Motulsky. Copyright 1995-96 by GraphPad Software. 3-4

[24] Motulsky HJ. Neubig RR. Analyzing Binding Data. 2010 *Curr Protoc Neurosci*; 52:7.5.1-7.5.65

[25] Davenport AP, Russell FD. Radioligand Binding Assays: Theory and Practice. Current Directions in Radiopharmaceutical Research and Development. 1996 *Developments in Nuclear Medicine*; 30:169-79

[26] Competitive binding experiments. In: The GraphPad Guide to Analyzing Radioligand Binding Data. Dr. Harvey Motulsky. Copyright 1995-96 by GraphPad Software. 6-9

[27] Cheng Y. Prusoff WH. Relationship between the inhibition constant (K1) and the concentration of inhibitor which causes 50 per cent inhibition (I50) of an enzymatic reaction. 1973 *Biochem Pharmacol*; 22:3099-108

[28] Qume M. Overview of Ligand- Receptor Binding Techniques. In: Mary Keen. Methods in Molecular Biology Volume 106. Receptor Binding Techniques. 1999, 3-23

[29] Harvester Operation and Service Manual Brandel®

[30] http://www.perkinelmer.com/resources/technicalresources/applicationsupportknowledgebase/radiometric/filter_ligand.xhtml (10.03.2014)

[31] Calculations with Radioactivity. In: The GraphPad Guide to Analyzing Radioligand Binding Data, Motulsky H, 16-18

8 APPENDIX

TECHNICAL DATA SHEET

Membrane Target Systems™

Caution: For Laboratory Use. A research reagent for research purposes only

human Adenosine A_3 Receptor

Product No.: ES-012-M400UA

Lot No.: 1651032

Material Provided

Membranes:	1 x 400 units / 400 µL frozen aliquot

Product Information

Cellular Background:	CHO-K1
GenBank Accession Number:	L22607
Unit Size:	1.5 µg protein / unit
Storage Buffer:	50 mM Tris-HCL (pH 7.4), 0.5mM EDTA, 10mM $MgCl_2$, 10% sucrose.
Storage Conditions:	Store at -80°C. **Freeze-thaw is not recommended** as it can affect product performance and homogeneity. In order to minimize negative impact of freeze-thawing, flash freeze in liquid nitrogen for 30 seconds prior to transferring to -80°C.
Stability:	This product is stable for at least 3 years from reception if used and stored under recommended conditions.

Quality Control

Bmax and Kd are determined using radioactive saturation binding assays (Figure 1). Protein concentration is determined using the BCA method [1]. Ratio-to-Reference (RTR) is determined by dividing the maximal signal of the current lot (Bmax in fmoles) by the maximal signal of a pre-defined reference tested in parallel. RTR is an indicator of lot-to-lot consistency. *We certify that these results meet our quality release criteria.

Ratio-to-Reference (RTR):	0.82
Expression Level (B_{MAX}):	2.6 pmol/mg membrane protein.
K_D for [^{125}I]-AB-MECA:	0.78 nM
Protein Concentration:	1.5 µg/µL

*(1) Smith, P.K., et al. (1985). Anal. Biochem. **150**, 76-85.*

PerkinElmer
For the Better

Recommended Assay Conditions

Assay Buffer: 25 mM Hepes pH 7.4, 10 mM $MgCl_2$, 1 mM $CaCl_2$, 0.5% BSA

Wash Buffer: 50 mM Tris-HCl pH 7.4

Binding Protocol: Binding assays are performed in 200 µL total volume according to the following conditions:

1 - Membrane dilution: 0.05 mL of membranes + 7.45 mL assay buffer (1:150 dilution)

2 - Incubation: 25 µL of incubation buffer or IB-MECA (Sigma I146) 250 µM final for non specific binding (Saturation binding assay)

For competition binding assay: 25 µL of reference compounds at decreasing concentrations (see figure 2)

25 µL of radioligand at the appropriate concentration (see graph below)
150 µL of diluted membranes

3 - Incubation time: 60 minutes at 27 °C

4 - Filtration: aspirate and wash 9 x 500 µL with ice cold wash buffer over GF/C filter (presoaked in 0.5 % BSA).

Lot Specific Data

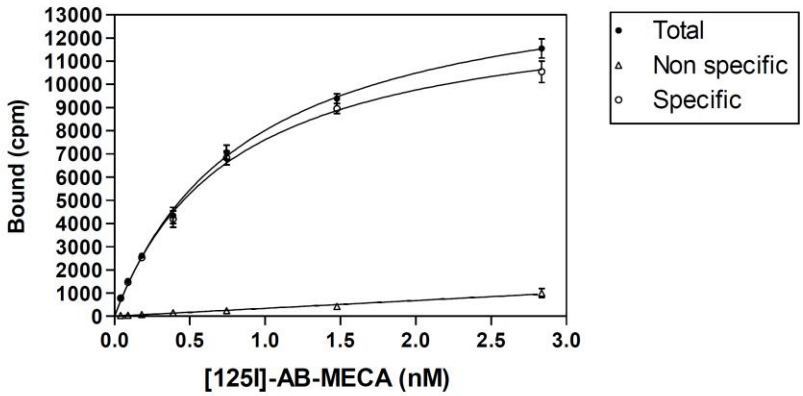

Figure 1: Saturation binding assay curve (filtration)
96-well saturation binding assay curve (1.5 µg membranes/well, TopCount®) using [^{125}I]-AB-MECA (PerkinElmer NEX312 Lot No.: GU91420)

Typical Product Data

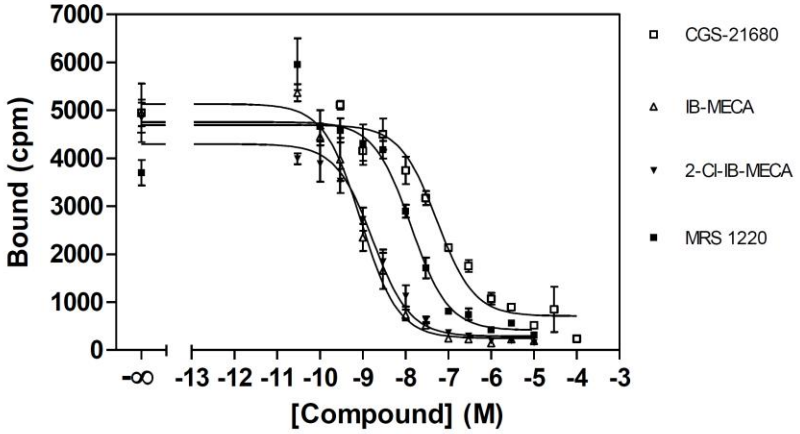

Figure 2: Competition binding assay curve (filtration)
96-well competition binding assay curve (1.5 µg membranes/well, TopCount®). Recommended radioligand concentration = 0.4 nM.

*Even though two sites can be observed occasionally with some ligands, the data presented is derived from single site fitting.

Reference Compounds	Ki (nM)
CGS-21680	43
IB-MECA	0.73
2-Cl-IB-MECA	1.4
MRS 1220	11

Suggested Materials and Instrumentation

Please visit our website

www.perkinelmer.com/GPCR

This product is not for resale or distribution except by authorized distributors.

When applicable, the CMV promoter is covered by U.S. Patents 5,168,062 and 5,385,839, licensed to PerkinElmer by the University of Iowa research Foundation

LIMITED WARRANTY: PerkinElmer BioSignal Inc. warrants that, at the time of shipment, the products sold by it are free from defects in material and workmanship and conform to specifications which accompany the product. PerkinElmer BioSignal Inc. makes no other warranty, express or implied with respect to the products, including any warranty of merchantability or fitness for any particular purpose. Notification of any breach of warranty must be made within 60 days of receipt unless otherwise provided in writing by PerkinElmer BioSignal Inc. No claim shall be honored if the customer fails to notify PerkinElmer BioSignal Inc. within the period specified. The sole and exclusive remedy of the customer for any liability of PerkinElmer BioSignal Inc. of any kind including liability based upon warranty (express or implied whether contained herein or elsewhere), strict liability contract or otherwise is limited to the replacement of the goods or the refunds of the invoice price of goods. PerkinElmer BioSignal Inc. shall not in any case be liable for special, incidental or consequential damages of any kind.

PerkinElmer, Inc.
940 Winter Street
Waltham, MA 02451 USA
P: (800) 762-4000 or
(+1) 203-925-4602
www.perkinelmer.com

PerkinElmer®

For a complete listing of our global offices, visit www.perkinelmer.com/ContactUs

TECHNICAL DATA SHEET

Membrane Target Systems™

Caution: For Laboratory Use. A research reagent for research purposes only

human Adenosine A_{2A} Receptor

Product No.: RBHA2AM400UA

Lot No.: 1650615

Material Provided

Membranes:	1 x 400 units / 400 µL frozen aliquot

Product Information

Cellular Background:	HEK293
GenBank Accession Number:	NM_000675
Unit Size:	9 µg protein / unit
Storage Buffer:	50 mM Tris-HCL (pH 7.4), 0.5mM EDTA, 10mM $MgCl_2$, 10% sucrose.
Storage Conditions:	Store at -80°C. **Freeze-thaw is not recommended** as it can affect product performance and homogeneity. In order to minimize negative impact of freeze-thawing, flash freeze in liquid nitrogen for 30 seconds prior to transferring to -80°C.
Stability:	This product is stable for at least 3 years from reception if used and stored under recommended conditions.

Quality Control

Bmax and Kd are determined using radioactive saturation binding assays (Figure 1). Protein concentration is determined using the BCA method [(1)]. Ratio-to-Reference (RTR) is determined by dividing the maximal signal of the current lot (Bmax in fmoles) by the maximal signal of a pre-defined reference tested in parallel. RTR is an indicator of lot-to-lot consistency. *We certify that these results meet our quality release criteria.

Ratio-to-Reference (RTR):	1.1
Expression Level (B_{MAX}):	12 pmol/mg membrane protein.
K_D for [^{3}H]-CGS 21680:	23 nM
Protein Concentration:	9 µg/µL

*(1) Smith, P.K., et al. (1985). Anal. Biochem. **150**, 76-85.*

PerkinElmer
For the Better

Recommended Assay Conditions

Assay Buffer: 50 mM Tris-HCl pH 7.4, 10 mM $MgCl_2$, 1 mM EDTA, 1 µg/mL Adenosine Deaminase

Wash Buffer: 50 mM Tris-HCl pH 7.4, 154 mM NaCl

Binding Protocol: Binding assays are performed in 550 µL total volume according to the following conditions:

1 - Membrane dilution: 0.05 mL of membranes + 24.95 mL assay buffer (1:500 dilution)

2 - Incubation: 25 µL of incubation buffer or 5′-(N-Ethylcarboxamido)adenosine (Sigma E2387) 50 µM final for non specific binding (Saturation binding assay)

For competition binding assay: 25 µL of reference compounds at decreasing concentrations (see figure 2)

25 µL of radioligand at the appropriate concentration (see graph below)
500 µL of diluted membranes

3 - Incubation time: 90 minutes at 27 °C

4 - Filtration: aspirate and wash 9 x 500 µL with ice cold wash buffer over GF/C filter (presoaked in 0.5 % PEI).

Lot Specific Data

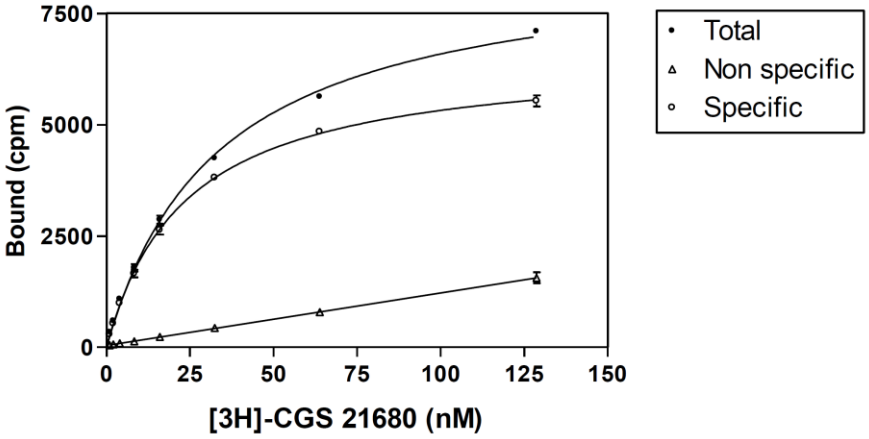

Figure 1: Saturation binding assay curve (filtration)
96-well saturation binding assay curve (9 µg membranes/well, TopCount®) using [^{3}H]-CGS 21680 (PerkinElmer NET1021 Lot No.: 619326)

PerkinElmer
For the Better

Typical Product Data

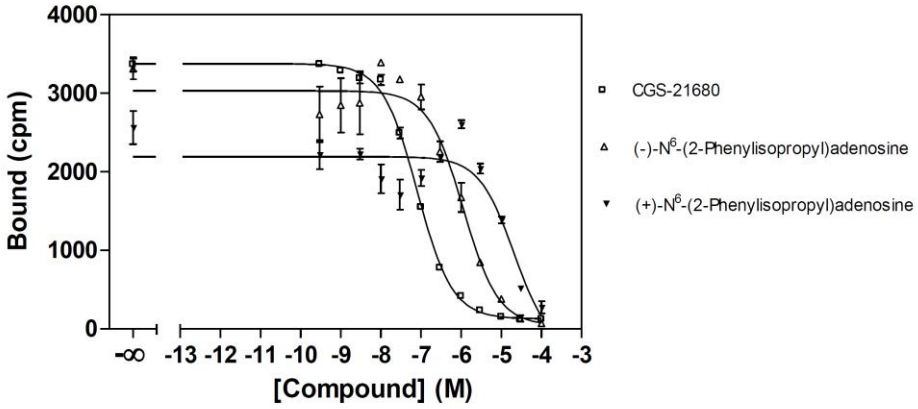

Figure 2: Competition binding assay curve (filtration)
96-well competition binding assay curve (9 µg membranes/well, TopCount®). Recommended radioligand concentration = 50 nM.

*Even though two sites can be observed occasionally with some ligands, the data presented is derived from single site fitting.

Reference Compounds	Ki (nM)
CGS-21680	47
(−)-N^6-(2-Phenylisopropyl)adenosine	658
(+)-N^6-(2-Phenylisopropyl)adenosine	12073

PerkinElmer
For the Better

Suggested Materials and Instrumentation

Please visit our website

www.perkinelmer.com/GPCR

This product is not for resale or distribution except by authorized distributors.

LIMITED WARRANTY: PerkinElmer BioSignal Inc. warrants that, at the time of shipment, the products sold by it are free from defects in material and workmanship and conform to specifications which accompany the product. PerkinElmer BioSignal Inc. makes no other warranty, express or implied with respect to the products, including any warranty of merchantability or fitness for any particular purpose. Notification of any breach of warranty must be made within 60 days of receipt unless otherwise provided in writing by PerkinElmer BioSignal Inc. No claim shall be honored if the customer fails to notify PerkinElmer BioSignal Inc. within the period specified. The sole and exclusive remedy of the customer for any liability of PerkinElmer BioSignal Inc. of any kind including liability based upon warranty (express or implied whether contained herein or elsewhere), strict liability contract or otherwise is limited to the replacement of the goods or the refunds of the invoice price of goods. PerkinElmer BioSignal Inc. shall not in any case be liable for special, incidental or consequential damages of any kind.

PerkinElmer, Inc.
940 Winter Street
Waltham, MA 02451 USA
P: (800) 762-4000 or
(+1) 203-925-4602
www.perkinelmer.com

PerkinElmer®

For a complete listing of our global offices, visit www.perkinelmer.com/ContactUs

TECHNICAL DATA SHEET

Membrane Target Systems™

Caution: For Laboratory Use. A research reagent for research purposes only

human Adenosine A_1 Receptor

Product No.: ES-010-M400UA

Lot No.: 1719064

Material Provided

Membranes: 1 x 400 units / 400 µL frozen aliquot

Product Information

Cellular Background: CHO-K1

GenBank Accession Number: NM_000674

Unit Size: 10 µg protein / unit

Storage Buffer: 50 mM Tris-HCL (pH 7.4), 0.5mM EDTA, 10mM $MgCl_2$, 10% sucrose.

Storage Conditions: Store at -80°C. **Freeze-thaw is not recommended** as it can affect product performance and homogeneity. In order to minimize negative impact of freeze-thawing, flash freeze in liquid nitrogen for 30 seconds prior to transferring to -80°C.

Stability: This product is stable for at least 3 years from reception if used and stored under recommended conditions.

Quality Control

Bmax and Kd are determined using radioactive saturation binding assays (Figure 1). Protein concentration is determined using the BCA method [(1)]. Ratio-to-Reference (RTR) is determined by dividing the maximal signal of the current lot (Bmax in fmoles) by the maximal signal of a pre-defined reference tested in parallel. RTR is an indicator of lot-to-lot consistency. *We certify that these results meet our quality release criteria.

Ratio-to-Reference (RTR): 1.4

Expression Level (B_{MAX}): 3.6 pmol/mg membrane protein.

K_D for [^{3}H]-Cyclopentyl-1,3-dipropylxanthine : 1.7 nM

Protein Concentration: 10 µg/µL

*(1) Smith, P.K., et al. (1985). Anal. Biochem. **150**, 76-85.*

PerkinElmer
For the Better

Recommended Assay Conditions

Assay Buffer: 25 mM Hepes pH 7.4, 5 mM $MgCl_2$, 1 mM $CaCl_2$, 100 mM NaCl

Wash Buffer: 25 mM Hepes pH 7.4, 5 mM $MgCl_2$, 1 mM $CaCl_2$, 100 mM NaCl

Binding Protocol: Binding assays are performed in 550 µL total volume according to the following conditions:

1 - Membrane dilution: 0.05 mL of membranes + 24.95 mL assay buffer (1:500 dilution)

2 - Incubation: 25 µL of incubation buffer or 8-Cyclopentyl-1,3-dipropylxanthine (Sigma C101) 10 µM final for non specific binding (Saturation binding assay)

For competition binding assay: 25 µL of reference compounds at decreasing concentrations (see figure 2)

25 µL of radioligand at the appropriate concentration (see graph below)
500 µL of diluted membranes

3 - Incubation time: 60 minutes at 27 °C

4 - Filtration: aspirate and wash 9 x 500 µL with ice cold wash buffer over GF/B filter (presoaked in 0.5 % PEI).

Lot Specific Data

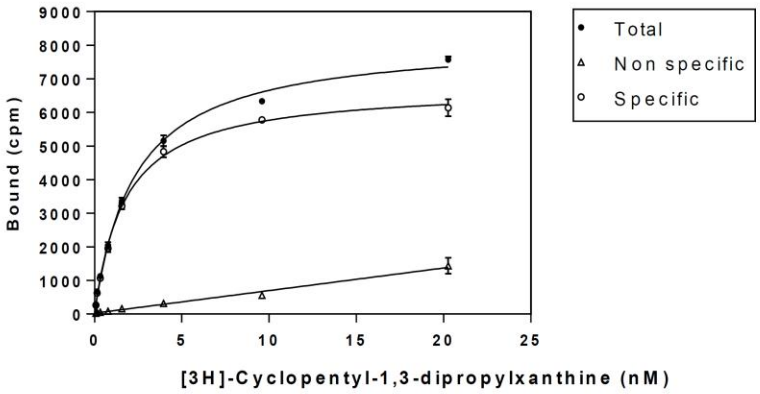

Figure 1: Saturation binding assay curve (filtration)
96-well saturation binding assay curve (10 µg membranes/well, TopCount®) using [^{3}H]-Cyclopentyl-1,3-dipropylxanthine (PerkinElmer NET974 Lot No.: 1656280)

PerkinElmer
For the Better

Typical Product Data

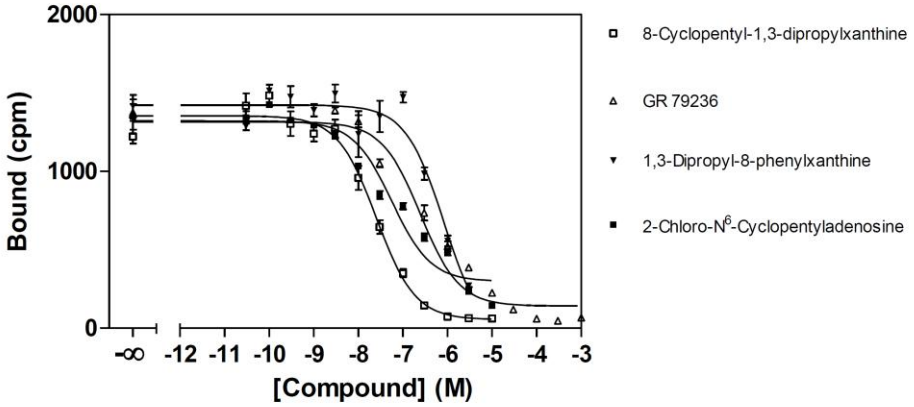

Figure 2: Competition binding assay curve (filtration)
96-well competition binding assay curve (10 µg membranes/well, TopCount®). Recommended radioligand concentration = 1.7 nM.

*Even though two sites can be observed occasionally with some ligands, the data presented is derived from single site fitting.

Reference Compounds	Ki (nM)
8-Cyclopentyl-1,3-dipropylxanthine	17
GR 79236	165
1,3-Dipropyl-8-phenylxanthine	576
2-Chloro-N^6-Cyclopentyladenosine	38

PerkinElmer
For the Better

Suggested Materials and Instrumentation

Please visit our website

www.perkinelmer.com/GPCR

This product is not for resale or distribution except by authorized distributors.

When applicable, the CMV promoter is covered by U.S. Patents 5,168,062 and 5,385,839, licensed to PerkinElmer by the University of Iowa research Foundation

LIMITED WARRANTY: PerkinElmer BioSignal Inc. warrants that, at the time of shipment, the products sold by it are free from defects in material and workmanship and conform to specifications which accompany the product. PerkinElmer BioSignal Inc. makes no other warranty, express or implied with respect to the products, including any warranty of merchantability or fitness for any particular purpose. Notification of any breach of warranty must be made within 60 days of receipt unless otherwise provided in writing by PerkinElmer BioSignal Inc. No claim shall be honored if the customer fails to notify PerkinElmer BioSignal Inc. within the period specified. The sole and exclusive remedy of the customer for any liability of PerkinElmer BioSignal Inc. of any kind including liability based upon warranty (express or implied whether contained herein or elsewhere), strict liability contract or otherwise is limited to the replacement of the goods or the refunds of the invoice price of goods. PerkinElmer BioSignal Inc. shall not in any case be liable for special, incidental or consequential damages of any kind.

PerkinElmer, Inc.
940 Winter Street
Waltham, MA 02451 USA
P: (800) 762-4000 or
(+1) 203-925-4602
www.perkinelmer.com

PerkinElmer®

For a complete listing of our global offices, visit www.perkinelmer.com/ContactUs

TECHNICAL DATA SHEET ^{3}H

Caution: For Laboratory Use. A product for research purposes only.

8-CYCLOPENTYL-1,3-DIPROPYLXANTHINE, [DIPROPYL-2,3-^{3}H(N)]-

Product Number: NET974

LOT SPECIFIC INFORMATION

Lot Number:	1749715
Specific Activity:	120.0 Ci/mmol
	4440.0 GBq/mmol
Production Date:	25 April 2013

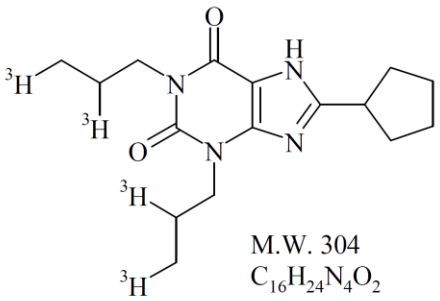

M.W. 304
$C_{16}H_{24}N_4O_2$

PACKAGING: 1 mCi/ml (37 MBq/ml) in ethanol, under nitrogen in a silanized vial. Shipped in dry ice.

STABILITY AND STORAGE RECOMMENDATIONS: The stability of 8-cyclopentyl-1,3-dipropylxanthine, [dipropyl-2,3-^{3}H(N)]- is currently being evaluated. Initial studies indicate that when 8-cyclopentyl1,3-dipropylxanthine, [dipropyl-2,3-^{3}H(N)]- is stored at -20°C in its original solvent and at its original concentration, the rate of decomposition is initially 3% for 6 months. Stability is nonlinear and not correlated to isotope half-life. Lot to lot variation may occur.

SPECIFIC ACTIVITY RANGE: 80-120 Ci/mmol (2960-4440 GBq/mmol)

RADIOCHEMICAL PURITY: This product was initially found to be greater than 97% when determined by the following methods. The rate of decomposition can accelerate. It is advisable to check purity prior to use:

High pressure liquid chromatography on a Zorbax ODS column using the following mobile phase:
1% triethylamine acetate pH 4.0 : acetonitrile, (1:1).

Thin layer chromatography on silica gel using the following solvent system:
toluene : ethyl acetate : diethylamine, (8:2:0.2).

QUALITY CONTROL: The radiochemical purity of 8-cyclopentyl-1,3-dipropylxanthine, [dipropyl2,3-^{3}H(N)]- is checked at appropriate intervals using the first listed chromatography method.

PREPARATIVE PROCEDURE: 8-Cyclopentyl-1,3-dipropylxanthine, [dipropyl-2,3-^{3}H(N)]- is prepared by the catalytic reduction of an appropriate precursor. The product is purified by HPLC.

HAZARD INFORMATION: WARNING: This product contains a chemical known to the state of California to cause cancer.

PerkinElmer, Inc.
549 Albany Street
Boston, MA 02118 USA
P: (800) 762-4000 or (+1) 203-925-4602
www.perkinelmer.com/nenradiochemicals
For a complete listing of our global offices, visit www.perkinelmer.com/ContactUs

PerkinElmer®

TECHNICAL DATA SHEET

^{3}H

Caution: For Laboratory Use. A product for research purposes only.

CGS 21680, [CARBOXYETHYL-^{3}H(N)]-

Product Number: NET1021

LOT SPECIFIC INFORMATION

Lot Number:	1651413
Specific Activity:	36.05 Ci/mmol
	1334 GBq/mmol
Production Date:	13-Sep-2012

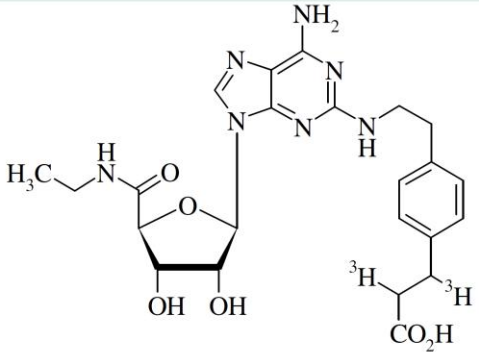

M.W. 499
$C_{23}H_{29}N_7O_6$

PACKAGING: 1 mCi/ml (37 MBq/ml) in 70% ethanol, under argon, in a silanized vial. Shipped in dry ice.

STABILITY AND STORAGE RECOMMENDATIONS: The stability of CGS 21680, [carboxyethyl-^{3}H(N)]- is currently being evaluated. Initial studies indicate that when CGS 21680, [carboxyethyl-^{3}H(N)]- is stored at -20°C in its original solvent and at its original concentration, the rate of decomposition is initially 1% for 3 months from date of purification. Stability is nonlinear and not correlated to isotope half-life.

SPECIFIC ACTIVITY RANGE: 30-60 Ci/mmol (1110-2220 GBq/mmol)

RADIOCHEMICAL PURITY: This product was initially found to be greater than 97% when determined by the following method. The rate of decomposition can accelerate. It is advisable to check purity prior to use:

High pressure liquid chromatography on a Vydac Proteins and Peptides C_{18} column using the following mobile phase:
0.2% trifluoroacetic acid : acetonitrile, (80:20).

QUALITY CONTROL: The radiochemical purity of CGS 21680, [carboxyethyl-^{3}H(N)]- is checked at appropriate intervals using the listed chromatography method.

REFERENCES:

1. Williams, M. et al., *FASEB Journal*, Vol. 3A 1047 (1986).
2. Hutchison, A. et. al., *J. Pharmacol. Exp. Ther.*, 251(1), 47 (1989).
3. Jarvis, M. et. al., *J. Pharmacrol. Exp. Ther.*, 251(3), 888 (1989).

HAZARD INFORMATION: WARNING: This product contains a chemical known to the state of California to cause cancer.

PerkinElmer, Inc.
549 Albany Street
Boston, MA 02118 USA
P: (800) 762-4000 or (+1) 203-925-4602
www.perkinelmer.com/nenradiochemicals
For a complete listing of our global offices, visit www.perkinelmer.com/ContactUs

PerkinElmer®

TECHNICAL DATA SHEET

^{125}I

Caution: For Laboratory Use. A product for research purposes only.

[^{125}I]-4-AMINOBENZYL-5'-N-METHYLCARBOXAMIDEOADENOSINE

Product Number: NEX312

[^{125}I]-AB-MECA

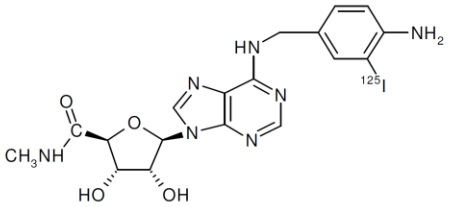

LOT SPECIFIC INFORMATION

CALCULATED AS OF: 9-Sep-2013

LOT NUMBER: GU01830

SPECIFIC ACTIVITY: 81.4 TBq/mmol
2200 Ci/mmol
156 MBq/µg
4207 µCi/µg

CONCENTRATION: 6.38 MBq/ml
172.5 uCi/ml

RADIOCHEMICAL PURITY: ≥ 95%

MOLECULAR WEIGHT: 523

Package Size Information

Package Size as of 18-Oct-2013	Volume
370 kBq 10 uCi	0.100 mL
1.85 MBq 50 µCi	0.500 mL

PACKAGING: [^{125}I]-AB-MECA is in methanol (may contain up to 2% acetonitrile from the purification process). It is shipped ambient.

STABILITY AND STORAGE: [^{125}I]-AB-MECA should be stored at 4°C or lower. Under these conditions the product is stable and usable for at least six weeks after fresh lot date.

SPECIFIC ACTIVITY: The initial specific activity of [^{125}I]-AB-MECA is 2200 Ci/mmol, (81 TBq/mmol), 4207 µCi/µg (156 MBq/µg). Preparative HPLC separates unlabeled AB-MECA from [^{125}I]-AB-MECA. Upon decay, [^{125}I]-AB-MECA undergoes decay catastrophe and the specific activity remains constant with time. However, it is not known what molecular fragments are generated from the decay event or what functional activity these fragments may have in different assays. References on ^{125}I decay and decay catastrophe of ^{125}I labeled compounds are available.[1-5]

RADIOCHEMICAL PURITY: Initially greater than 95% radiochemically pure as determined by HPLC.

PREPARATIVE PROCEDURE: AB-MECA is radioiodinated with no carrier added ^{125}I using a modification of the Hunter and Greenwood method[6] and is purified by reversed phase HPLC.

AVAILABILITY: [^{125}I]-AB-MECA is routinely available from stock and is prepared fresh and packaged for shipment on the second Monday of each month. Please inquire for larger package sizes.

APPLICATIONS: Agonist ^{125}I-AB-MECA binds strongly to cloned, human A_3AR (type 3 adenosine receptors): K_d=0.59.[7,8] However, ^{125}I-AB-MECA lacks high selectivity for A_3AR, so blocking agents for A_1AR (type 1 adenosine receptors) may greatly improve autoradiography results. A_3AR ligand

HAZARD WARNING: This product contains a chemical (s) known to the state of California to cause cancer. This product also contains a component which is harmful by contact or ingestion. It is irritating to the eyes and skin. It is toxic and flammable. The target organs are the eyes, the central nervous system, the kidneys and the liver.

RADIATION UNSHIELDED: 280mR/hr/mCi at vial surface.

REFERENCES:

1. Doyle, V.M., Buhler, F.R., Burgisser, E., *Eur. J. Pharm.* 99 353 (1984).
2. Schmidt, J., *J. Biol. Chem.* 259 1160 (1984).
3. Loring, R.H., Jones, S.W., Matthews-Bellinger, J., Salpeter, M.M., *J. Biol. Chem.* 257 1418 (1982).
4. Berridge, M.S., Jiang, V.W., Welch, M.J., *Rad. Res.* 82 467 (1980).
5. Charlton, D.E., *Rad. Res.* 107 163 (1986).
6. Hunter, W.M. and Greenwood, F.C., *Nature* 194 495 (1962).
7. Olah, M.E., Gallo-Rodriguez, C., Jacobson, K.A., Stiles, G.L., *Mol. Pharm.* 45 978-82 (1994).
8. Ji, X., *et al.*, *J. Med Chem.* 39 781-8 (1996).
9. Jacobson, K.A., Pannell, L.K., Ji, X.D., Jarvis, M.F., Williams, M., Hutchinson, A.J., Barrington, W.W., Stiles,
10. Barrington, W.W., Jacobson, K.A., Hutchinson, A.J., Williams, M., Stiles, G.L., *Proc. Nat'l. Acad. Sci.* *USA* 86

IODINE-125 DECAY CHART HALF LIFE=60 days

Radiations: Gamma 35.5 keV (7%) , X-ray K alpha 27 KeV (112%), K beta 31 keV (24%)

DAYS	0	2	4	6	8	10	12	14	16	18
0	1.000	0.977	0.955	0.933	0.912	0.891	0.871	0.851	0.831	0.812
20	0.794	0.776	0.758	0.741	0.724	0.707	0.691	0.675	0.660	0.645
40	0.630	0.616	0.602	0.588	0.574	0.561	0.548	0.536	0.524	0.512
60	0.500	0.489	0.477	0.467	0.456	0.445	0.435	0.425	0.416	0.406
80	0.397	0.388	0.379	0.370	0.362	0.354	0.345	0.338	0.330	0.322
100	0.315	0.308	0.301	0.294	0.287	0.281	0.274	0.268	0.262	0.256
120	0.250	0.244	0.239	0.233	0.228	0.223	0.218	0.213	0.208	0.203

To obtain the correct radioactive concentration or amount for a date before the calibration date: divide by the decay factor corresponding to the number of days before the calibration date. To obtain the correct radioactive concentration or amount for a date after the calibration date: multiply by the decay factor corresponding to the number of days after the calibration date.

PerkinElmer, Inc.
Boston, MA 02118 USA
Phone: (800) 762-4000 or
(+1) 203-925-4602
www.perkinelmer.com

PerkinElmer

For a complete listing of our global offices, visit www.perkinelmer.com/lasoffices

Theresa BALBER

Personal Information

- Nationality: Austria
- Place of birth: Vienna

Education

2007 - 2014 University of Vienna
Study of Pharmacy

1999 - 2007 High School
Neusprachliches Realgymnasium, Mödling

1995 - 1999 Elementary School
Volksschule, Laxenburg

Professional experience

2010, 2011 Water & Waste
Internship, environmental chemistry

2012-2014 Pharmacy
Central Apotheke, Wr. Neudorf

Languages

German: native

English: fluent spoken and written (Cambridge University Certificate Advanced)

French: basic knowledge

Spanish: basic knowledge

Personal Interests

Reading, Swimming, Snowboarding